Submitted in Support of the U.S. Navy’s 2025 Annual Marine Species Monitoring Report for the Pacific

Distribution and Occurrence of Southern Resident Killer Whales and Chinook Salmon on the Outer Coast of Washington State from 2018-2024

Joshua D. Stewart[1], P. Santiago Domínguez-Sánchez[1], Candice K. Emmons[2], M. Bradley Hanson[2], Marla M. Holt[2], Doug Jackson[3], Alyssa Lopez[1], Hannah J. Myers[4], Hannah L. Sawyer[1], Kathleen M. Stafford[1], David D. Huff[2]

[1]Marine Mammal Institute, Oregon State University
[2]Northwest Fisheries Science Center, NOAA Fisheries
[3]QEDA Consulting
[4]University of Alaska Fairbanks

Photo Credit: Astrid van Ginneken, Center for Whale Research

Suggested citation: J.D. Stewart, P.S. Dominguez-Sanchez, C.K. Emmons, D. Jackson, M.B. Hanson, M.M. Holt, A. Lopez, H.J. Myers, H.L. Sawyer, K.M. Stafford, D.D. Huff. Distribution and occurrence of Southern Resident killer whales and Chinook salmon on the outer coast of Washington State from 2018-2024. Prepared for: U.S. Navy, U.S. Pacific Fleet, Pearl Harbor, Hawaii. Prepared by: Oregon State University under MIPR N0007024MP0ERWL and Cooperative Agreement #G24AC00556; and NOAA Northwest Fisheries Science Center under MIPR N00070-21-MP-0EQ8Q. April 2026.

Submitted in Support of the U.S. Navy's 2025 Annual Marine Species Monitoring Report for the Pacific

REPORT DOCUMENTATION PAGE

Form Approved
OMB No. 0704-0188

1. REPORT DATE *(DD-MM-YYYY)*
04-2026

2. REPORT TYPE
Monitoring report

3. DATES COVERED *(From - To)*
2018–2024

4. TITLE AND SUBTITLE
DISTRIBUTION AND OCCURRENCE OF SOUTHERN RESIDENT KILLER WHALES AND CHINOOKE SALMON ON THE OUTER COAST OF WASHINGTON STATE FROM 2018-2024

5a. CONTRACT NUMBER

5b. GRANT NUMBER

5c. PROGRAM ELEMENT NUMBER

6. AUTHOR(S)
Joshua D. Stewart
P. Santiago Domínguez-Sánchez
Candice K. Emmons
M. Bradley Hanson
Marla M. Holt
Doug Jackson
Alyssa Lopez
Hannah J. Myers
Hannah L. Sawyer
Kathleen M. Stafford
David D. Huff

5d. PROJECT NUMBER

5e. TASK NUMBER

5f. WORK UNIT NUMBER

7. PERFORMING ORGANIZATION NAME(S) AND ADDRESS(ES)
Marine Mammal Institute, Oregon State University
Northwest Fisheries Science Center, NOAA Fisheries
QEDA Consulting
University of Alaska Fairbanks

8. PERFORMING ORGANIZATION REPORT NUMBER

9. SPONSORING/MONITORING AGENCY NAME(S) AND ADDRESS(ES)
Commander, U.S.Pacific Fleet, 250 Makalapa Dr. Pearl Harbor, HI

10. SPONSOR/MONITOR'S ACRONYM(S)

11. SPONSORING/MONITORING AGENCY REPORT NUMBER

12. DISTRIBUTION AVAILABILITY STATEMENT
Approved for public release; distribution is unlimited

13. SUPPLEMENTARY NOTES

14. ABSTRACT
From 2018 to 2024, a coordinated acoustic monitoring program was conducted along the outer coast of Washington State to quantify the spatial and seasonal occurrence of Southern Resident killer whales (SRKW) and acoustically tagged Chinook salmon in areas overlapping U.S. Navy training and testing activities. Monitoring was carried out through complementary efforts led by NOAA Fisheries' Marine Mammal Ecology Team (MMET), the Salmon Ocean Behavior and Distribution (SOBAD) project, and Oregon State University (OSU). The monitoring network consisted of passive acoustic moorings deployed from the mouth of the Columbia River to Cape Flattery, with additional offshore coverage west of the Strait of Juan de Fuca. Hydrophones were used to detect SRKW vocalizations, while 69 kHz acoustic receivers recorded detections of tagged Chinook salmon. Array design and sampling intensity varied across years in response to evolving research objectives, but near continuous coverage of the Washington coast was maintained throughout the study period.
Between 2019 and 2024, the Chinook salmon telemetry program collected 101,026 receiver-days of effort. A total of 498 Chinook salmon were acoustically tagged in Alaska and along the U.S. West Coast, of which 238 individuals were detected on the Washington coast array, resulting in 4,269 daily detection events. Tagged salmon represented multiple

genetic stock aggregates, with Interior Ocean-type Chinook comprising the largest proportion of detections. The highest detection rates of Chinook salmon generally occurred during spring and summer. Chinook exhibited elevated use of the north-central Washington coast, the Strait of Juan de Fuca, and, in some years, the southern coast near the Columbia River. Spatiotemporal models revealed substantial interannual variability in Chinook occurrence patterns, likely reflecting differences in stock composition of tagged individuals and oceanographic conditions.
From 2018 to 2024, MMET hydrophones recorded 8,305 days of acoustic effort across five core sites and detected SRKW on 900 recording-days. In 2023 and 2024, SOBAD and OSU hydrophones added 5,016 days of effort across 15 sites, with SRKW detected on 378 recording-days. SRKW were detected most frequently at northern sites near the Strait of Juan de Fuca and Swiftsure Bank, where mean detection rates during summer reached approximately 2–5 days per week. Across all years, SRKW occurrence peaked consistently from July through November in the northern portion of the study area. On the southern Washington coast near the Columbia River mouth, SRKW detections were infrequent and occurred primarily during early spring. Spatiotemporal modeling showed a stable seasonal pattern across years, with highest occurrence in the far north during summer and early fall and lower, but persistent, winter presence.

15. SUBJECT TERMS
Monitoring, satellite tagging, Chinook salmon, Southern resident killer whales, endangered species, Northwest Traning Range Complex, Washington Coast

16. SECURITY CLASSIFICATION OF:			17. LIMITATION OF ABSTRACT	18. NUMBER OF PAGES	19a. NAME OF RESPONSIBLE PERSON
			UU	45	5Department of the Navy
a. REPORT	**b. ABSTRACT**	**c. THIS PAGE**			**19b. TELEPONE NUMBER (*Include area code)***
Unclassified	Unclassified	Unclassified			808-471-6391

Executive Summary

From 2018 to 2024, a coordinated acoustic monitoring program was conducted along the outer coast of Washington State to quantify the spatial and seasonal occurrence of Southern Resident killer whales (SRKW) and acoustically tagged Chinook salmon in areas overlapping U.S. Navy training and testing activities. Monitoring was carried out through complementary efforts led by NOAA Fisheries' Marine Mammal Ecology Team (MMET), the Salmon Ocean Behavior and Distribution (SOBAD) project, and Oregon State University (OSU). The monitoring network consisted of passive acoustic moorings deployed from the mouth of the Columbia River to Cape Flattery, with additional offshore coverage west of the Strait of Juan de Fuca. Hydrophones were used to detect SRKW vocalizations, while 69 kHz acoustic receivers recorded detections of tagged Chinook salmon. Array design and sampling intensity varied across years in response to evolving research objectives, but near continuous coverage of the Washington coast was maintained throughout the study period.

Between 2019 and 2024, the Chinook salmon telemetry program collected 101,026 receiver-days of effort. A total of 498 Chinook salmon were acoustically tagged in Alaska and along the U.S. West Coast, of which 238 individuals were detected on the Washington coast array, resulting in 4,269 daily detection events. Tagged salmon represented multiple genetic stock aggregates, with Interior Ocean-type Chinook comprising the largest proportion of detections. The highest detection rates of Chinook salmon generally occurred during spring and summer. Chinook exhibited elevated use of the north-central Washington coast, the Strait of Juan de Fuca, and, in some years, the southern coast near the Columbia River. Spatiotemporal models revealed substantial interannual variability in Chinook occurrence patterns, likely reflecting differences in stock composition of tagged individuals and oceanographic conditions.

From 2018 to 2024, MMET hydrophones recorded 8,305 days of acoustic effort across five core sites and detected SRKW on 900 recording-days. In 2023 and 2024, SOBAD and OSU hydrophones added 5,016 days of effort across 15 sites, with SRKW detected on 378 recording-days. SRKW were detected most frequently at northern sites near the Strait of Juan de Fuca and Swiftsure Bank, where mean detection rates during summer reached approximately 2–5 days per week. Across all years, SRKW occurrence peaked consistently from July through November in the northern portion of the study area. On the southern Washington coast near the Columbia River mouth, SRKW detections were infrequent and occurred primarily during early spring. Spatiotemporal modeling showed a stable seasonal pattern across years, with highest occurrence in the far north during summer and early fall and lower, but persistent, winter presence.

Table of Contents

Table of Acronyms **5**

1. Background & History of Monitoring Effort **6**

1.1 MMET Monitoring 2018 – 2024 7

1.2 SOBAD Monitoring 2019 – 2024 8

1.3 OSU Monitoring 2024 8

2. Methods **10**

2.1 Chinook Salmon Acoustic Tag Deployments 10

2.2 Acoustic Telemetry Receivers 13

2.3 Chinook Data Processing & Statistical Model 14

2.4 Passive Acoustic Monitoring for SRKW 18

2.5 SRKW Data Processing & Statistical Model 23

3. Results **27**

3.1 Chinook Tagging Stock Composition 27

3.2 Chinook Detection Overview 28

3.2 Chinook Spatial Modeling Results 30

3.4 SRKW Detection Overview 35

3.5 SRKW Spatial Modeling Results 35

4. Acknowledgments **40**

5. References **40**

Table of Acronyms

ESA	Endangered Species Act
ESU	Evolutionarily Significant Unit
IOOS	Integrated Ocean Observing System
ISSM	Inshore Surface Mooring
LTSA	Long-Term Spectral Average
MMPA	Marine Mammal Protection Act
MMET	Marine Mammal Ecology Team
NANOOS	Northwest Association of Networked Ocean Observing Systems
NOAA	National Oceanic and Atmospheric Administration
NWFSC	Northwest Fisheries Science Center's
NWTTSA	Northwest Training and Testing Study Area
OCNMS	Olympic Coast National Marine Sanctuary
OOI	Ocean Observatories Initiative
OSU	Oregon State University
PAM	passive acoustic monitoring
SHSM	CE07 Shelf Surface Mooring
SOBAD	Salmon Ocean Behavior and Distribution
SRKW	Southern Resident killer whales

1. Background & History of Monitoring Effort

The U.S. Navy conducts military training and testing in Pacific Northwest waters to ensure its forces are combat-ready, while NOAA Fisheries oversees the protection of threatened and endangered marine species and issues permits to the Navy under the Endangered Species Act (ESA) and the Marine Mammal Protection Act (MMPA). The Navy's Marine Species Monitoring Program, linked to these permits, seeks to understand how Southern Resident killer whales (*Orcinus orca ater*; SRKW) and certain Evolutionarily Significant Units (ESUs) of Chinook salmon (*Oncorhynchus tshawytscha*), both ESA-listed, share habitats. Since 2014, the Navy has supported the NOAA Northwest Fisheries Science Center (NWFSC) Marine Mammal Ecology Team's (MMET) research to map the SRKW's offshore distribution and identify essential habitats. Beginning in 2018, the Navy also sponsored the NWFSC's Salmon Ocean Behavior and Distribution (SOBAD) project to track the offshore distribution of Chinook salmon. Beginning in 2024, the Navy sponsored Oregon State University (OSU) to maintain an array of acoustic moorings to track the occurrence of SRKW and detections of fish tagged with acoustic transmitters, including Chinook salmon, on the outer coast of Washington. This report summarizes the work of these three projects during 2018-2024, when monitoring efforts for both SRKW and tagged Chinook salmon were ongoing.

The SRKW population has declined by ~25% since 1995, and the current size of the population (as of July 2025) is 74 individuals (Center for Whale Research 2026). Research to support SRKW recovery includes investigating the impacts of noise and disturbance (Holt et al. 2021, Tennessen et al. 2024), pollution and contaminants (Krahn et al. 2009), food availability, and recently, genetic inbreeding (Kardos et al., 2023, National Marine Fisheries Service 2008). SRKW preferentially select Chinook salmon as prey (Ford et al. 2006, Krahn et al. 2007, Hanson et al. 2010, Wasser et al. 2017, Hanson et al., 2021, Van Cise et al. 2024), and widespread declines in Chinook salmon abundance may constrain SRKW recovery via reduced birthrates and increased mortality (Ward et al. 2009, Ford et al. 2010, Stewart et al. 2021). Chinook salmon populations utilize the west coast of Vancouver Island and Washington State coastal habitats during their migration and marine habitat occupancy. Efforts to minimize harvest impacts on depleted populations are complicated by differences among populations in when and how they use these habitats (e.g., shelf resident vs. highly migratory life history strategies). Furthermore, ecosystem-based management in the region requires accounting for variability in the spatiotemporal availability of Chinook salmon as prey for SRKW. Yet, our understanding of predator-prey interactions in marine shelf habitats is limited. Thus, management actions to recover at-risk Chinook salmon populations and provide adequate prey for resident-type killer whales will benefit from understanding when and where salmon and killer whales are distributed.

The movement patterns of the three SRKW pods (J, K and L) are complex and seasonally driven. K and L pods engage in more extensive travel along the North American west coast, with movements extending from central California to the northern waters of British Columbia, while J pod's coastal distribution remains comparatively closer to, and within, the Salish Sea, Puget Sound, and inland waters of Washington and British Columbia (Hanson et al. 2017). All three SRKW pods have historically spent the majority of the summer months in the Salish Sea, targeting Chinook salmon returning to the Fraser River and Puget Sound tributaries (Olson et al. 2018). In recent years, SRKW occupancy of these inland water habitats have declined during the summer, possibly in response to declining prey availability (Ettinger et al. 2022; Stewart et al. 2023). Use of the outer coast habitat along Washington state and Vancouver Island is therefore most likely increasing, but distribution, occupancy, and prey availability in these regions is relatively limited (see Olesen and Hildebrand 2012, Hanson et al. 2013, Riera et al. 2019) not well studied. Passive acoustic monitoring has been pivotal in providing insights into the SRKWs' distribution and behavior, particularly along the broader west coast of North America (Hanson et al. 2013). This acoustic data, collected through an array of hydrophones, is valuable for understanding the SRKWs' use of the Northwest Testing and Training (NWTT) range site, an important training area for the U.S. Navy, and surrounding areas (Hanson et al. 2017). This study seeks to provide a more comprehensive understanding of SRKW seasonal movements and occupancy patterns along the outer coast of Washington state, and the seasonal distribution and availability of Chinook salmon prey, assisting with the development of effective conservation strategies.

1.1 MMET Monitoring 2018 – 2024

The MMET SRKW monitoring program has focused on the long-term occurrence of SRKW at several focal sites along the Washington coast (Figure 1). Passive acoustic monitoring (PAM) devices were deployed at Swiftsure Bank and the western end of the Strait of Juan de Fuca, an area that is a known SRKW feeding hotspot (DFO 2025) during the summer months. In addition, PAM moorings were placed at three locations along the outer coast of Washington State (La Push, Westport, and the Columbia River mouth). Moorings were serviced once per year in the summer and therefore had duty-cycled recording intervals to allow sufficient battery life and storage space for year-round recording. Additional passive acoustic receivers were deployed in Oregon and California but are not included in this report given its focus on the Washington Coast.

1.2 SOBAD Monitoring 2019 – 2024

The SOBAD program was initially focused on the distribution of Chinook salmon on the outer coast of Washington State. Chinook salmon were captured in Southeast Alaska and along the coast of Washington and implanted with acoustic tags that produce individually coded pings that stationary 69 kHz acoustic receivers can identify and record. Tagged fish were then released. Acoustic receiver moorings were deployed along the coast of Washington State in high densities from 2019 to 2022 to capture high-resolution movements of Chinook salmon along the coast and across the continental shelf. The array layout changed substantially across years to address different ecological monitoring objectives; those layouts are presented in maps in the Results section. In 2023, the SOBAD project began deploying PAM recorders on moorings, enabling each mooring station to detect SRKW vocalizations and Chinook acoustic tags simultaneously. The array design changed during this period to emphasize full spatial coverage along the Washington coast, but at a lower spatial resolution than 2019 to 2022. A single latitudinal line of moorings was deployed along the coast from the mouth of the Columbia River to Cape Flattery, focused on the 50m isobath. In addition, a longitudinal line of moorings was deployed from Cape Flattery to ~ 50km offshore. PAM recorders were programmed to record continuously rather than duty-cycled, and as a result, moorings were recovered and redeployed three times per year in spring, summer, and fall.

1.3 OSU Monitoring 2024

Beginning in 2024, OSU took over management of the 69 kHz acoustic receiver and PAM mooring array along the Washington coast, while continuing to co-lead the research program with the SOBAD project. The array design implemented by the SOBAD project in 2023 (a latitudinal line from the Columbia River to Cape Flattery on the 50m isobath, and a longitudinal array offshore of Cape Flattery) was maintained for 2024.

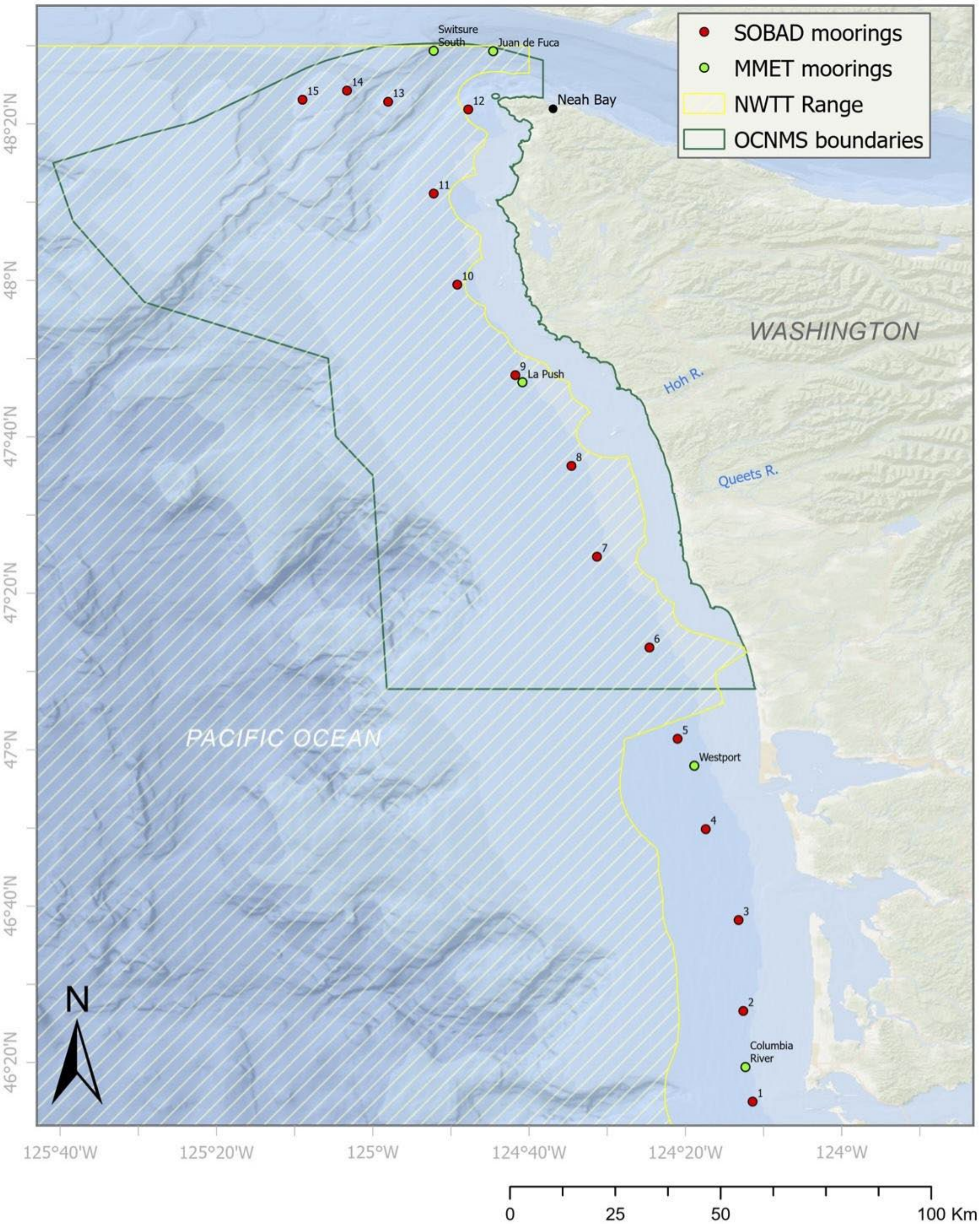

Figure 1. Acoustic mooring stations along the coast of Washington State in 2024, in relation to the Northwest Testing and Training (NWTT) Range and the Olympic Coast National Marine Sanctuary (OCNMS). SOBAD mooring stations are shown in Red; MMET stations are shown in Green. Note that the location of acoustic moorings, including many additional 69 kHz moorings, has changed each year from 2018 to 2024. Annual mooring configurations for SoundTraps and 69 kHz receivers are shown in Figures 3 and 5.

2. Methods

2.1 Chinook Salmon Acoustic Tag Deployments

From 2019 through 2024, Chinook salmon detected on the Washington Coast acoustic receiver array originated from multiple tagging efforts conducted by NOAA Fisheries, Oregon State University, and collaborating programs operating across a broad geographic range. These efforts included fish captured and explicitly tagged for this project, as well as fish tagged in prior years and under other studies whose detections were recorded opportunistically as they transited the array and for which complete tag metadata were available. Tagging locations varied among years and included coastal marine waters off Washington State and offshore regions of the Gulf of Alaska (Figure 2). Genetic stock identification was used to assign tagged individuals to stock aggregates with similar life-history characteristics, ocean entry timing, and geographic origin; stock aggregation and assignment procedures are described below.

Across all tagging efforts summarized here, Chinook salmon were captured using hook-and-line in marine waters. They were surgically implanted with InnovaSea 69 kHz acoustic transmitter tags programmed to random ping rates between 1 ping every 60 and 120 seconds. Captured fish primarily represented juvenile and sub-adult Chinook salmon; life stage was inferred post-capture based on fork length rather than used as a capture criterion. Fish were immediately placed into an anesthetic bath (25 mg/L AQUI-S® 20E) until reaching stage III anesthesia, defined as total loss of equilibrium and no response to tactile stimuli (typically ~4 minutes). The use of AQUI-S® 20E was conducted under INAD permit #11-47. Once anesthetized, fork length (nearest cm) was measured, scales were collected from the preferred standardized area posterior to the dorsal fin and above the lateral line for age determination, and an anal-fin clip was taken for genetic analysis.

Transmitters were implanted via a 10–15 mm ventral incision made with a sterile scalpel. The acoustic transmitter and a passive integrated transponder (PIT) tag, used for detection at freshwater monitoring locations such as dams, were inserted into the body cavity. The incision was closed with two or three simple interrupted surgeon's knots using Ethicon Y513 4-0 Monocryl suture and a 19 mm reverse-cutting needle, following established tagging guidelines (Smith et al. 2024). No explicit minimum size threshold was imposed; fish were selected based on suitability for surgical implantation of acoustic and PIT tags. Following surgery, fish were placed in a recovery tank supplied with fresh, aerated seawater until normal orientation and vigorous swimming were observed (generally 5–10 minutes), after which they were released near the capture location. The latitude, longitude, date, and time of release were recorded for each individual and are summarized by tagging location in Figure 2.

Tagged Chinook salmon with known origin tributaries based on genetic stock identification were grouped into stock aggregates to allow for sufficient sample sizes to model annual patterns of occurrence for stock aggregates with similar ocean entry timing and geographic origins. These stock aggregates were assigned based on life-history type, major geographic basin, and ocean-entry window (Table 1). The stock identification of some tagged individuals could not be determined, and the genetic stock identification results for individuals tagged in 2024 remain pending.

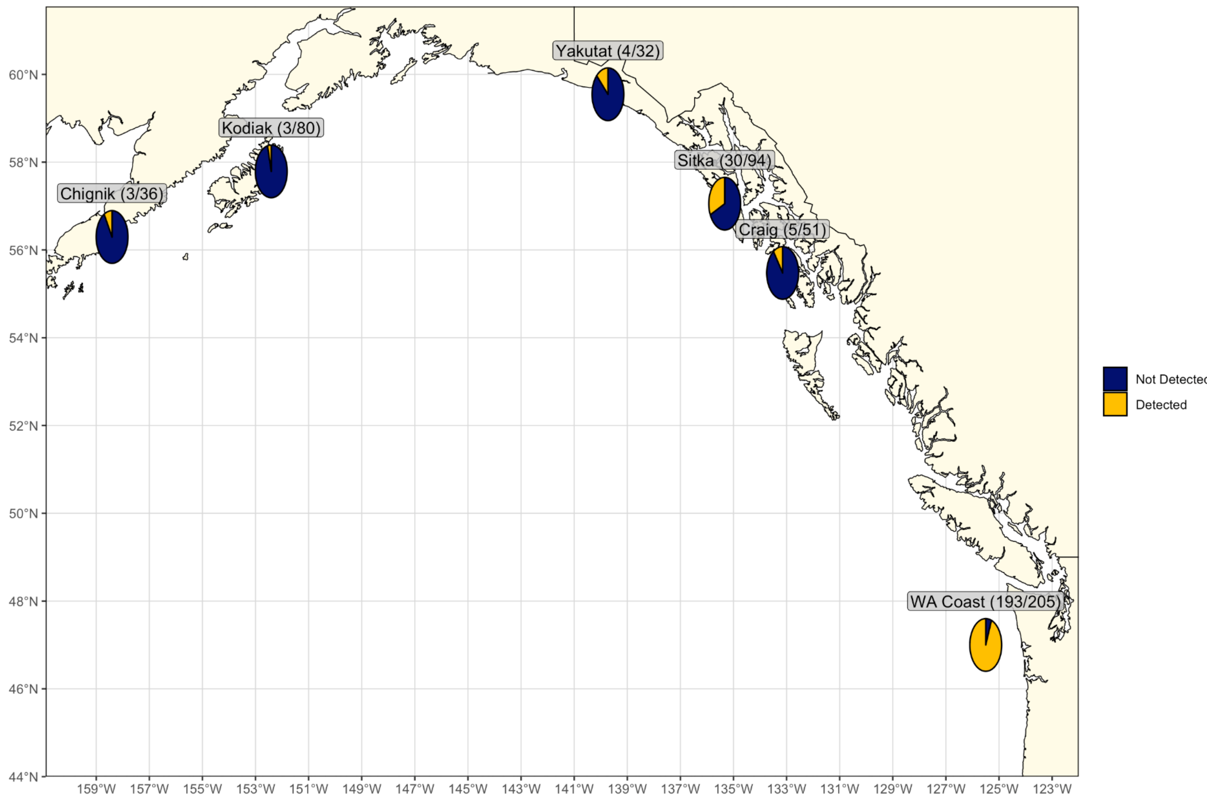

Figure 2. Deployment locations of 69 kHz acoustic tags in adult and sub-adult Chinook salmon. Pie charts indicate the proportion of tags deployed at each site that were detected at any point within the Washington coast acoustic array. The numbers in parentheses indicate (number detected / total number deployed) at each site.

Table 1. Chinook salmon stock aggregation table. Stock assignment of tagged salmon was based on genetic stock identification.

Stock Aggregate	Number of tags deployed	Stocks included	Rationale
Interior Ocean-type	147	Upper Columbia Summer/Fall, Deschutes Fall, Columbia (general), Columbia Spring	Subyearling (early) ocean entry from interior Columbia systems; rapid transition to coastal and offshore habitats; strong shelf migration northward into BC/AK.
Interior Stream-type	62	West Cascades Spring, Willamette Spring, South Thompson, Snake Spring	Late ocean entry (yearlings), stream-type freshwater rearing; strongest northward and Gulf of Alaska migration patterns with extensive offshore movement.
Oregon Coast	21	Mid- to North Coastal Oregon	Coastal Oregon fall populations; early ocean entry; prolonged California Current shelf use between Cape Mendocino and Washington; limited Alaska penetration.
Southern OR / Northern CA	2	Klamath, Rogue	Mixed but fall-dominated coastal stocks; early ocean entry; primary CCS residence south of Cape Bluff with occasional central CCS expansion.
California Central Valley	7	CA Central Valley	Ocean-type fall outmigrants from Central Valley; southern CCS residency (Monterey – Cape Mendocino); minimal northern migration relative to OR/WA stocks.
Puget Sound / WA Coast	3	Southern Puget Sound, Washington Coast, Strait of Juan de Fuca	Ocean-type fall origin; heavy inner Sound and WA-coastal utilization; moderate northward movement but notably less offshore and less Alaska-directed than interior river stocks.
Northern BC / Alaska	148	West Vancouver Island, East Vancouver Island, Northern British Columbia, Southeast Alaska	Ocean-type fall stocks from BC and AK outer/inner systems; early ocean entry; strong northern residency and sustained use of BC/AK shelf and Gulf of Alaska waters.
Undetermined	108		Genetic ID failed or is pending

2.2 Acoustic Telemetry Receivers

Innovasea 69 kHz acoustic receivers (model VR2AR) were deployed along the Washington Coast to detect tagged Chinook salmon. The density, locations, and orientation of the receiver array varied between years as research questions evolved. Annual receiver placements are detailed in Figure 3. While the design of the acoustic array changed year to year, coverage along the entire Washington Coast was maintained throughout the six-year study period. The SOBAD project maintained the majority of acoustic receivers. However, tag detections recorded on a small number of additional receivers were made available through the Ocean Tracking Network. Annual receiver deployment effort (i.e., periods with active receiver coverage) and standardized tag detections are shown by 0.1 degree latitude bins in Figure 4.

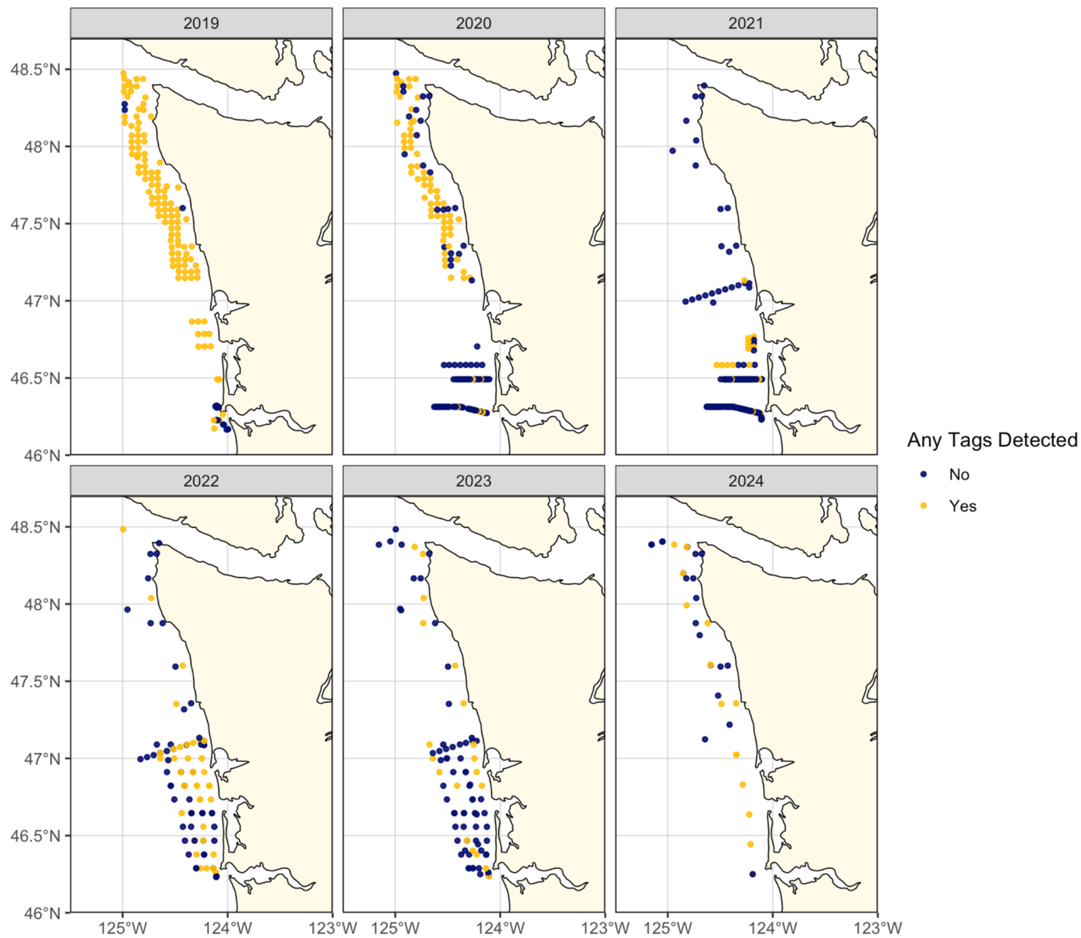

Figure 3. Map of 69 kHz acoustic receiver deployments by year, 2019-2024. Receivers include both SOBAD moorings and receivers with data posted to the Ocean Tracking Network. Mooring locations in blue did not detect any 69 kHz tags implanted in Chinook salmon during the indicated calendar year, whereas locations in yellow had one or more detections of tagged Chinook salmon during that calendar year. See Figure 4 for annual summaries of Chinook salmon tag detections by latitude.

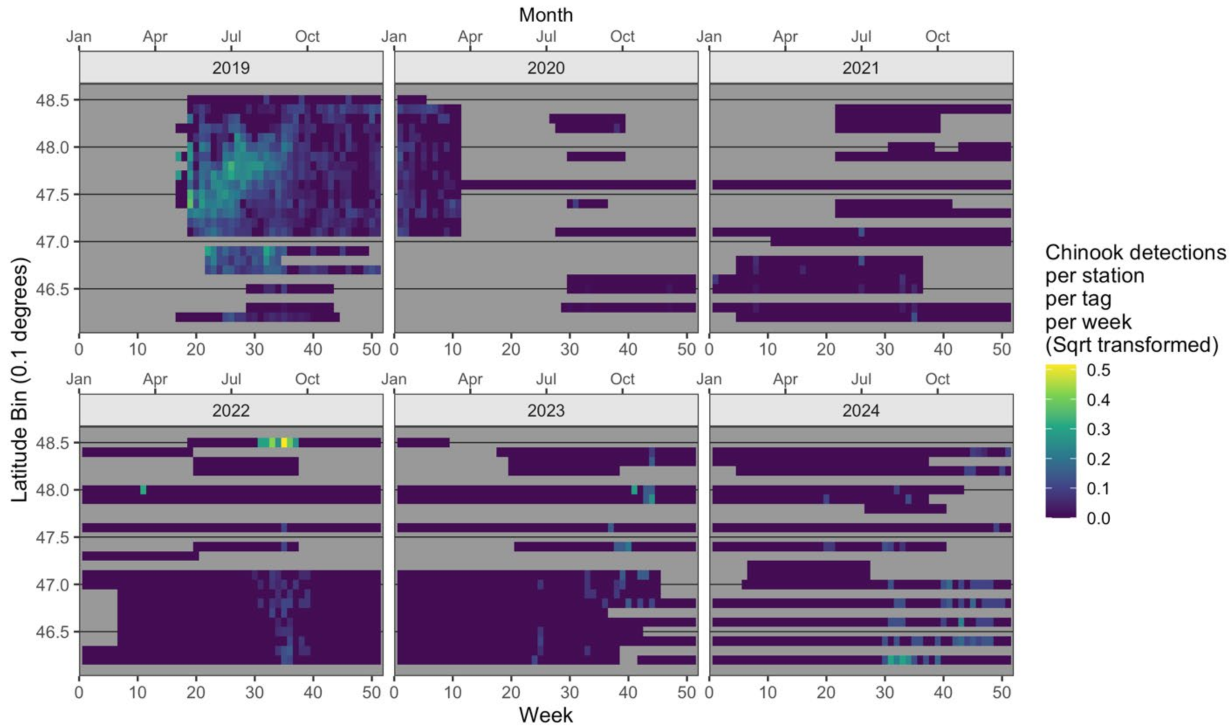

Figure 4. Standardized detection days of 69 kHz acoustic tags implanted in Chinook salmon, 2019-2024. Detections are standardized for effort by combining all active 69 kHz receivers into 0.1 degree latitudinal bins, and dividing the number of days with tag detections for each receiver within a latitudinal bin by the number of active receivers in that bin and the number of active tags for each calendar week. The resulting number of standardized detection days is then square-root transformed to improve the visibility of the detection gradient at lower values.

2.3 Chinook Data Processing & Statistical Model

Chinook tag data were modeled as daily presence or absence of individual tags at each receiver station to adequately account for both tagging effort and receiver coverage, both of which varied substantially across years. To prepare the tag detection database for this analysis, tag detections were first transformed into daily presence (1) or absence (0) on every acoustic receiver. A presence was any day with one or more detections of a given tag. Periods of absence were limited to dates between a tag's deployment date and the maximum tag duration for each tag type. Five tag types were deployed between 2019 and 2024: Innovasea V6, V7, V8, V9, and V16, each with a different expected maximum battery life. In addition, some tags had temperature and/or pressure sensors, which reduces expected battery life. We grouped tag deployments by tag model and sensors (e.g., V6, V9 Temperature, V9 Temperature+Pressure, V16) and determined the maximum duration between tag deployment and final tag detection for each category. We then added 30 days to this maximum value to avoid early truncation of the detection database. Using this maximum deployment duration, we populated the detection database with absences (0s) for each tag between the deployment date and the maximum duration for that tag type. These absences were applied to each acoustic receiver for each tag during the period when the receiver was deployed and active. This provided a final analysis database that included all recorded daily presences (1s) and all inferred absences (0s) for each tag on each receiver when both the tag and the receiver were active. Tags that were never detected on the Washington Coast array were excluded from this analysis.

Daily presence-absence data for tagged Chinook salmon at each station were used to estimate daily probability of occurrence along the Washington coast each year from 2019 to 2024 in a spatiotemporal generalized additive model (GAM) framework (Wood & Wood 2015). Daily presences were treated as 1's and absences as 0's; days with no active acoustic receivers were not included as observations in the model. A binomial response distribution was used to accommodate 0-1 data, with a logit link. Both model formulations estimated the probability of Chinook occurrence by latitude and day of the year (DOY; 1-365) each year, but the specific handling of these covariates was different among candidate models. Both candidate models used a tensor product to estimate a two-dimensional smoothed surface for latitude and DOY. In addition, both model formulations included random effects for each station. To avoid including hundreds of random effects for all unique acoustic receivers, receivers that were less than 1 km apart were assigned a shared station identifier for estimating random effects (but daily presence/absence detections from these receivers were not combined). Longitude was not included as an effect, as receivers were deployed primarily along a latitudinal gradient. We instead relied on station-level random effects to capture longitudinal variation in Chinook detection probabilities. To account for mortality and emigration from the study area, a smooth term was fit to the number of days since tag deployment in all candidate models. The primary difference between the candidate models was their handling of interannual variability. In the base model formulation (C_1), only a random effect of year was included, which would constrain the model to the same overall two-dimensional latitude–DOY occurrence pattern, but with higher or lower occurrence probabilities each year estimated by the random effect.

In the alternative model formulation (C_2), annual tensor products were estimated, meaning that the overall two-dimensional latitude – DOY occurrence patterns could be entirely different between years (Pedersen et al. 2019). Candidate models were fit using the mgcv package in R (Wood & Wood 2006, R Core Team 2024). Due to the large volume of input data, Fast Restricted Maximum Likelihood (fREML) was used to fit the models rather than the more common Restricted Maximum Likelihood (REML). Akaike information criterion (AIC) was used to select the model with the highest predictive performance. An overview of candidate model formulations used for Chinook tagging data is presented in Table 2.

To explore potential differences in ocean distribution by stock and life-history type, the above models were also fit to a subset of the tag detection database that included only tags from the Interior Ocean-type stock aggregate (models O1 & O2). Other stock aggregates did not have sufficient sample sizes of detected tags to run separate models.

Table 2. Description of candidate generalized additive models for Chinook tag spatiotemporal analysis (all tags combined). tp = tensor product; re = random effect; s = smooth term. The top model based on the AIC score is indicated with *.

Model	Effects Included	Deviance Explained	AIC
C_1	tp(Latitude, DOY) + re(Year) + re(Station) + s(Duration)	20.4%	58301.6
C_2	tp(Latitude, DOY) + tp(Latitude, DOY, by = Year, independent wiggliness) + re(Year) + re(Station) + s(Duration)	21%	**57858.9***

Table 3. Description of candidate generalized additive models for Interior Ocean-type Chinook tag spatiotemporal analysis. tp = tensor product; re = random effect; s = smooth term. The top model based on the AIC score is indicated with *.

Model	Effects Included	Deviance Explained	AIC
O_1	tp(Latitude, DOY) + re(Year) + re(Station) + s(Duration)	21.6%	43864
O_2	tp(Latitude, DOY) + tp(Latitude, DOY, by = Year) + re(Year) + re(Station) + s(Duration)	22%	**43634.4***

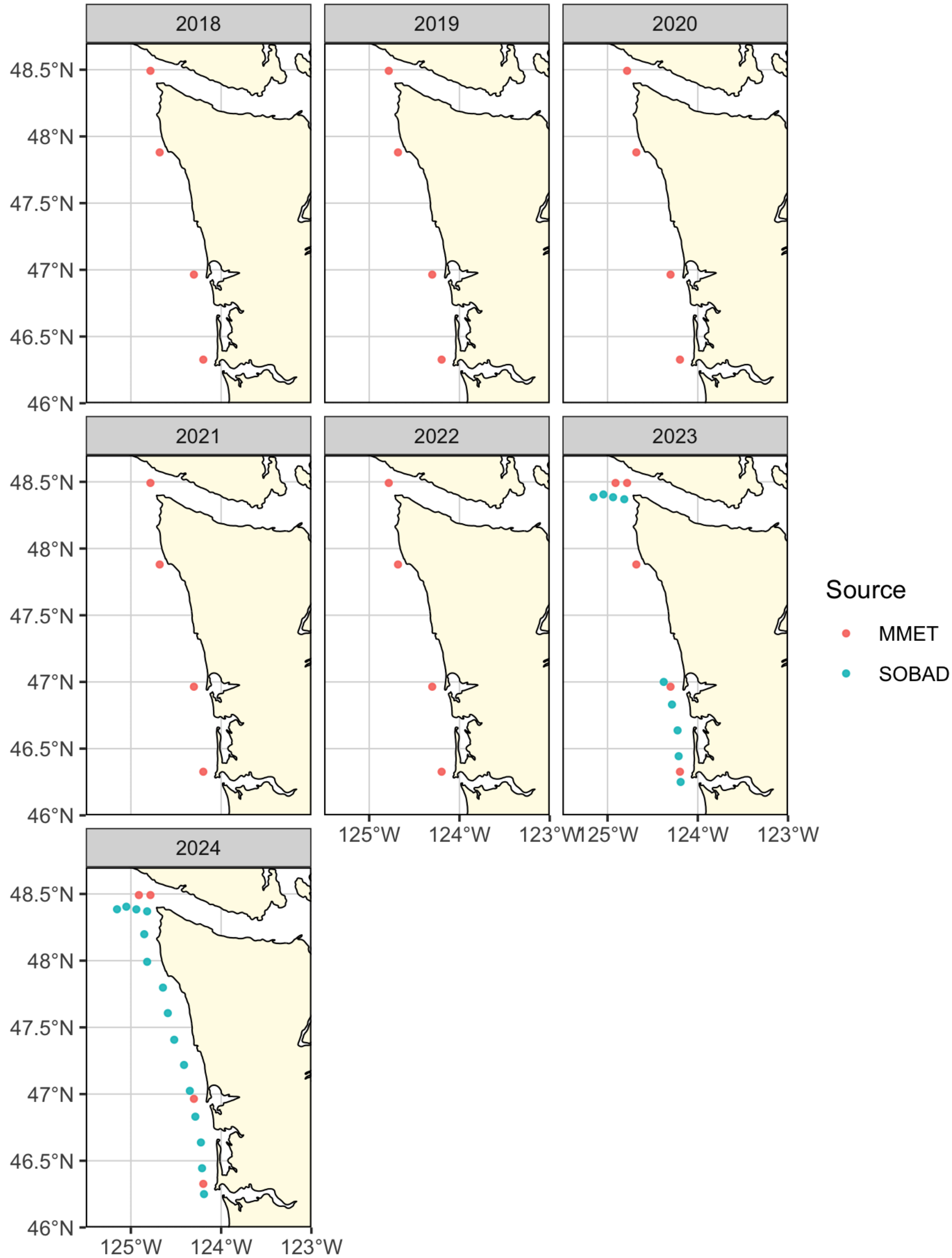

Figure 5. Map of SoundTrap passive acoustic mooring locations by year, 2018-2024. See Figures 7 and 8 for annual summaries of SRKW detections by station.

2.4 Passive Acoustic Monitoring for SRKW

2.4.1 MMET SoundTrap Programming & Manual SRKW Detection

Three types of autonomous passive acoustic recorders were deployed by MMET from 2018-2024: ecological acoustic recorders (EARs), SoundTrap 500STDs (ST500s) and SoundTrap 600STDs (ST600s). In summer 2018, the transition from EARs to ST500s was initiated and both an EAR and ST500 were deployed simultaneously at each location. The transition to ST600s began in summer 2022. EAR data were used after summer 2018 for analysis only when the ST500 failed.

EARs were programmed to record at a sampling rate of 25 kHz which provided 12.5 kHz of bandwidth. SoundTraps (ST500s and ST600s) were programmed to record at a sampling rate of 48 kHz providing 24 kHz of bandwidth. All recorder types were duty-cycled to record for 90 seconds every 10 minutes.

For each deployment 90 second recordings were sorted by day. EAR files were then concatenated and converted to wav files using a custom MATLAB (The MathWorks) script. Daily wav files were reviewed visually and aurally in either TRITON (Wiggins et al. 2010) for EAR data or Raven Pro for SoundTrap data, and the daily occurrence of all species detected was summarized (Emmons et al 2021). Those files containing killer whale sounds were further reviewed, and discrete calls were compared to a catalog of pod- and population-specific pulsed calls to determine the killer whale ecotype, population, clan (in the case of NRKW), and pod (if possible, in the case of SRKW) (Ford 1989).

2.4.2 SOBAD SoundTrap Programming & Notes on Mooring Design

SOBAD SoundTraps (Ocean Instruments model ST600STD) were programmed to record continuously, to maximize the detection probability of SRKW and other vocalizing marine mammals. From March to October 2023, SoundTraps were programmed to record with a sample rate of 192 kHz for an effective bandwidth monitored of 0.01-98 kHz. However, it was later determined that such a high sampling rate was not necessary to detect killer whale vocalizations. In addition, the extremely high sample rate substantially decreased battery life and increased the required storage capacity. Consequently, beginning in October 2023, SoundTraps were programmed to record at a 48 kHz sample rate for an effective bandwidth monitored of 0.01 to 24 kHz. Earlier audio recordings from March to October 2023 were decimated to the same 48 kHz sample rate to establish uniformity with later recordings for subsequent analysis. From October 2023 to February 2024, SOBAD SoundTraps were duty-cycled to record for 12 minutes every 20 minutes. All other SOBAD SoundTrap deployments had continuous recording.

In 2023 and 2024, moorings within the Olympic Coast National Marine Sanctuary (OCNMS) boundaries used a recoverable anchor design, which included an Innovasea Acoustic Release Canister (BARC model) with ~150 m of 3/8" dyneema line, and three 11" trawl floats, each providing ~8 kg of positive buoyancy. The Innovasea 69 kHz VR2AR receiver was integrated into the mooring design and served as the acoustic release, and the SoundTraps were affixed to the float package. In 2023, the BARC was connected to 70-90 kg of anchor material using stainless steel chain, whereas in 2024, the anchor tether was changed to 3/4" polypropylene line. Importantly, the collective >20 kg of positive buoyancy kept the tether from the BARC to the anchor material taut.

From March to June 2023, a mooring design with a non-recoverable anchor was used for the southern mooring stations outside of the OCNMS boundaries. This mooring design featured two 6" trawl floats, each providing ~2 kg of positive buoyancy. The 69 kHz VR2AR receiver served as the acoustic release, and the SoundTraps were affixed to it. The VR2AR receiver was tethered to ~100 lbs of anchor material using stainless steel chain. Due to insufficient positive buoyancy from the two 6" trawl floats, the recordings using this mooring design had excessive chain noise created by movement of the mooring as a result of wave action and currents. This chain noise precluded the use of automated SRKW detectors (described in the next section) on these data, as extensive mooring noise created an excessively high false positive detection rate in testing and validation exercises. We therefore used manual analysis of Long-Term Spectral Averages (LTSAs) in MATLAB's TRITON software package (Wiggins et al. 2010) to incorporate these data.

To eliminate chain noise interference, beginning in October 2023, moorings with non-recoverable anchors outside the OCNMS boundaries were converted to polypropylene line with a single 11" trawl float, with the 69 kHz VR2AR receiver serving as the acoustic release and the SoundTrap affixed to the polypropylene line approximately 8" above the VR2AR. A polypropylene line was used to connect the VR2AR to ~100 lbs of anchor material. This design largely eliminated mooring noise and was used for all deployments outside the OCNMS boundaries from October 2023 onwards.

2.4.3 Development, Testing, and Implementation of Automated SRKW Detection & Classification Pipeline

We developed a series of custom models to detect and classify SRKW and other marine mammals in the Washington Coast study area. First, we used a neural network to detect and classify seven classes of sounds present in the acoustic dataset: background noise, fish-eating killer whales (including both SRKW and Northern Resident killer whales [NRKW]), mammal-eating killer whales (*Orcinus orca* *rectipinnus*), humpback whales (*Megaptera novaeangliae*), Pacific white-sided dolphins (*Aethalodelphis obliquidens*), mooring noise, and vessel noise. Second, we used a logistic regression to predict the probability that an acoustic encounter of fish-eating killer whales was a true positive. Third, we developed a population-level neural network to classify high-probability fish-eating killer whale encounters as Southern Resident or Northern Resident. Each of these steps is described below.

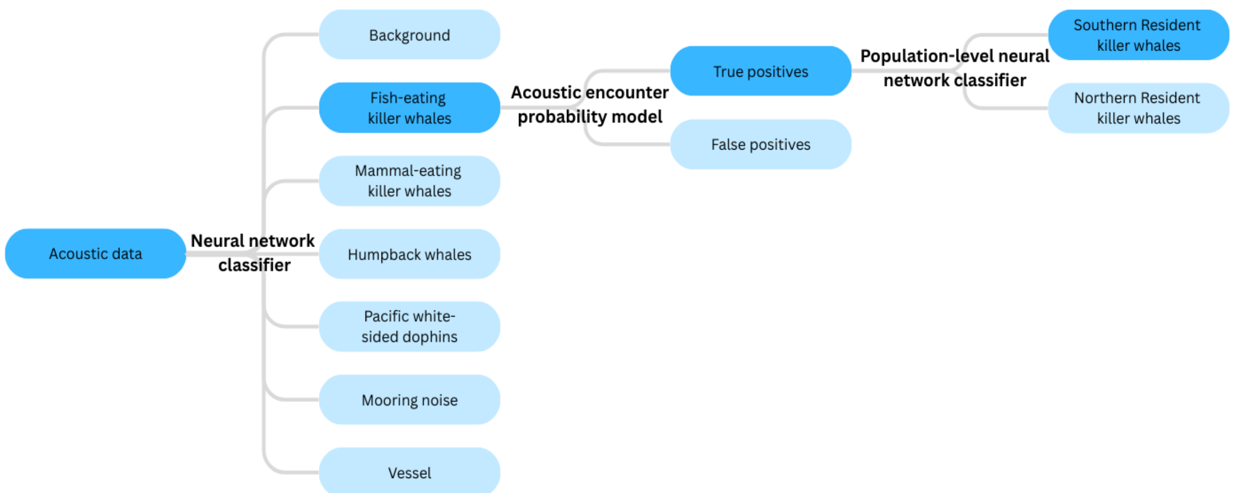

Figure 6. Acoustic detection and classification workflow, with steps to identify Southern Resident killer whales highlighted. Each node indicates a possible classification outcome of one of three models in the pipeline.

We utilized the open-source platform BirdNET (version 1.5.0; Kahl et al. 2021) to develop neural network classifiers for both the general acoustic data and fish-eating killer whale populations. The feature embeddings present in BirdNET enable few-shot transfer learning to other species, particularly those that vocalize in a similar frequency range (Ghani et al. 2023). BirdNET models are trained on three-second audio clips that include signals for each class. When the model is implemented to detect and classify sounds in an acoustic recording, BirdNET provides a confidence score[1] that indicates a trained model prediction of whether each three-second slice of the spectrogram contains a signal of a given class.

To develop training and testing datasets for the BirdNET model, we first searched LTSAs of acoustic data from all stations in the SOBAD array from May to October 2023 for marine mammal vocalizations. We then manually annotated the center points of signals in each class using Raven Pro (version 1.6.4; K. Lisa Yang Center for Conservation Bioacoustics 2023). A random value between -1 and 1 seconds was then

[1] Note that a confidence score is not equivalent to a probability score, and the relationship between confidence and probability is not strictly defined.

added to the center point, and a three-second clip was extracted centered on that point using the tuneR package (Ligges et al. 2023) in R (version 4.0.5; R Core Team 2024). This ensured that, when implemented on a recording, BirdNET would recognize signals that were not precisely centered within the three-second window. Clips were then randomly split into training and test datasets, with 80% of clips in each class used for training and 20% for model testing (Table 4). Models were trained using default parameters and the autotune setting in BirdNET, then evaluated on the test dataset. The model achieved 95 - 100% accuracy on all classes.

Table 4. Number of clips in training and test datasets for BirdNET neural network classifiers and model precision (true positives / (true positives + false positives) on the test dataset for each class.

Model	Class	Training data	Test data	Precision
All acoustic data	Background	220	56	0.980
	Fish-eating killer whales	1,350	428	0.977
	Mammal-eating killer whales	167	42	0.950
	Humpback whales	2,141	536	0.996
	Pacific white-sided dolphins	228	361	0.989
	Mooring noise	1,440	58	1.000
	Vessel	496	124	0.975
Population-level	Southern resident killer whales	6,080	1,521	1.000
	Northern resident killer whales	755	180	0.950

We implemented the custom BirdNET model for general acoustic detection and classification across all recordings from SOBAD hydrophone deployments from 2023 to 2024, except moorings at Stations 1-5 from March to June 2023, which suffered from excessive mooring chain noise as described in Section 2.4.2. We excluded all classifications with a confidence score less than 0.90. We grouped marine mammal classifications into "acoustic encounters," defined as periods with at least three 3-second windows classified as the same species with a break of no more than five minutes between classifications. For each acoustic encounter, we calculated the mean and median confidence scores, number of detections, encounter duration, detections per minute, and the proportion of detections with a confidence score greater than 0.99. For lower-priority marine mammal classes (mammal-eating killer whales, humpback whales, and Pacific white-sided dolphins), we reduced the probability of including false-positive encounters for each class by including only those with a mean confidence score in the 90th percentile or higher. We then summed the number of detection hours per day at each station.

For fish-eating killer whales, we developed a logistic regression model using encounter-level metrics to predict the probability that an acoustic encounter was a true positive. First, an experienced analyst manually reviewed 667 acoustic encounters classified as fish-eating killer whale vocalizations. A majority (68%) of encounters were false positives; however, false positive encounters were significantly shorter in duration than true fish-eating killer whale encounters (ANOVA, p = < 2e-16). On average, true positive fish-eating killer whale encounters lasted 36.93 min (s = 52.75, with encounters defined as above, with a break of no more than 5 min between detections). In contrast, the mean duration of false positive encounters was 11.87 min (s = 15.36). Logistic regression models were then built using all possible combinations of potential explanatory variables described above, excluding redundant variables (e.g., number of detections and detections per minute). Models were compared using AIC scores. The best model included mean confidence score, number of detections, encounter duration, and the proportion of detections with a confidence score greater than 0.99 (Table 5).

Table 5. Summary of model coefficients for the best logistic regression model predicting the probability that an acoustic encounter classified as fish-eating killer whales was a true positive.

Term	Estimate	Standard error	*p*
Intercept	-32.34	10.76	0.0027
Encounter duration	-0.03	0.01	0.0119
Mean confidence	31.74	11.29	0.0049
Number of detections	0.02	0.01	0.0006
Proportion of detections with confidence > 0.99	3.11	0.74	< 0.0001

We then applied this model to predict the probability that each acoustic encounter classified as fish-eating killer whales was a true positive. We filtered fish-eating killer whale encounters to include only those with a predicted true-positive probability greater than 0.90 and proceeded with the analysis. Including only encounters with a predicted true probability greater than 0.90 limits the predicted false-positive rate to less than 0.10.

Finally, we developed a second neural network in BirdNET to classify fish-eating killer whales into the Southern Resident and Northern Resident populations. As with the general BirdNET model, clips were manually annotated and extracted from our outer Washington coast dataset, as well as supplemented with manually annotated clips from a separately collected dataset in the northern Strait of Georgia (Pilkington et al. 2023) and the Northern Resident killer whale catalogue (Ford 1989). All clips were then randomly sorted into 80% training and 20% test datasets. The model achieved 95–100% precision on the test dataset (Table 4). We implemented this model across all SOBAD fish-eating killer whale encounters from 2023 to 2024 with a probability of at least 0.90 of being a true-positive encounter.

2.5 SRKW Data Processing & Statistical Model

SRKW detections from MMET and SOBAD moorings were independently binned into daily presences. Any days that had passive acoustic recording effort and no detections of SRKW were considered absences, although we note that it is possible in these cases that SRKW were within the detection range of the hydrophone but not vocalizing or missed by the automated detector-classifier when applied to the SOBAD mooring data. Raw weekly detections of SRKW (and graphical representations of recording effort) by MMET and SOBAD moorings from 2018 - 2024 are presented in Figure 7. Combined weekly detections of SRKW are presented in Figure 8.

Figure 7. Number of days per week with SRKW present for each hydrophone mooring along the Washington Coast, 2018-2024. The top panels represent MMET moorings, and the bottom panels represent SOBAD moorings. Gray periods indicate no recording effort. MMET mooring stations are indicated by letters (e.g., JF, SS, LP), and numbers indicate SOBAD mooring stations; see Figure 1 for a map of mooring locations. MMET and SOBAD stations within 10km of each other are listed on the same row (e.g., CR_1, WP_5). SOBAD stations 1 and 5 in 2023 (March – June) were manually reviewed for killer whale vocalizations, whereas all other SOBAD stations and recording periods were analyzed using automated SRKW detectors (see methods).

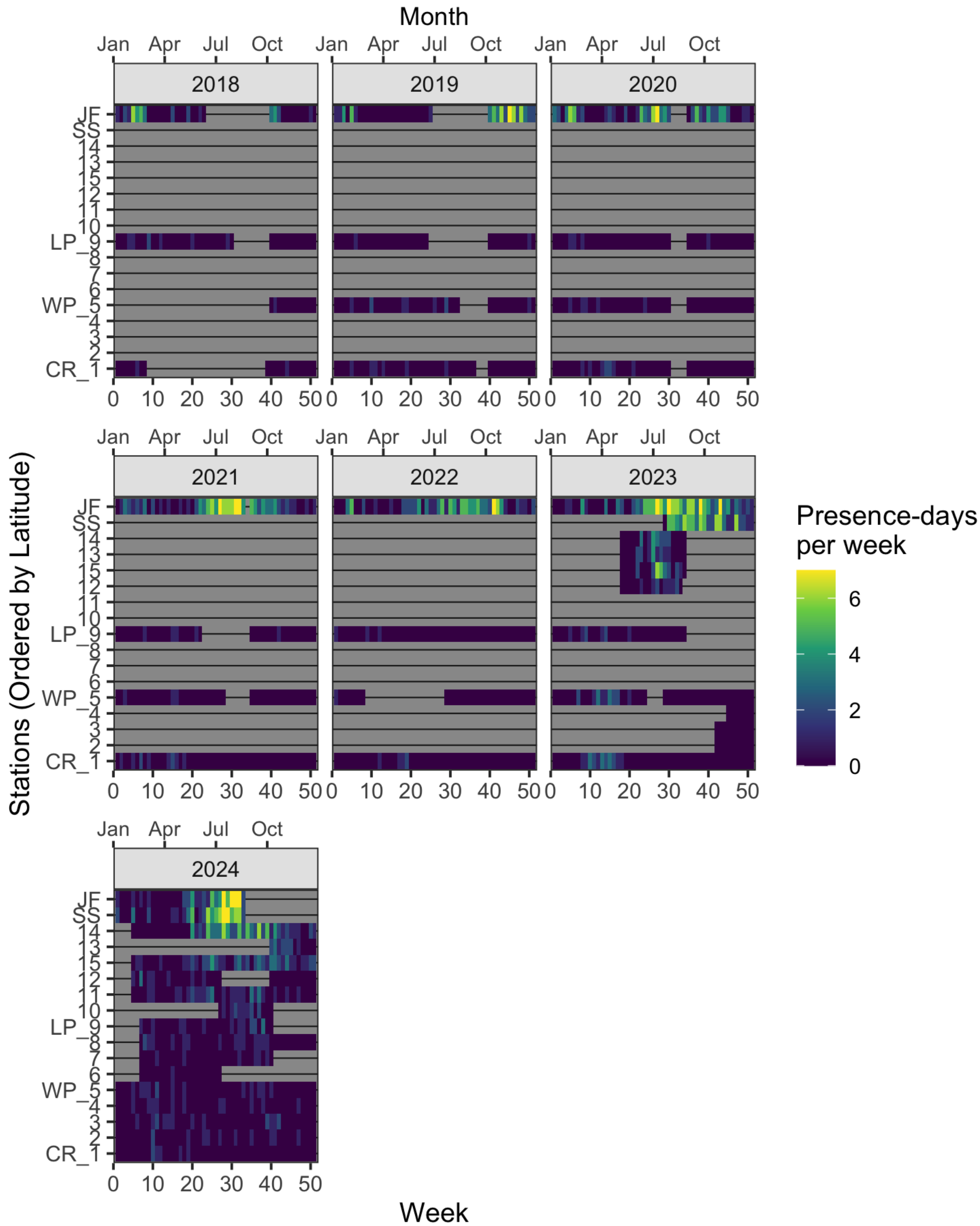

Figure 8. Number of days per week with SRKW present for each mooring along the Washington Coast, 2018-2024. Gray periods indicate no recording effort. MMET and SOBAD stations within 10km of each other were combined to represent weekly detection rates (e.g., CR_1, WP_5). MMET mooring stations are indicated by letters (e.g. JF, SS), and numbers indicate SOBAD mooring stations; see Figure 1 for a map of mooring locations.

Daily presence-absence data for SRKW at each station were used to estimate the daily probability of occurrence along the Washington coast each year from 2018 to 2024 in a spatiotemporal GAM framework, comparable to the Chinook tag analysis described above. Daily presences were treated as 1's and absences as 0's; days with no recording effort were not included as observations in the model. A binomial response distribution was used to accommodate 0-1 data, with a logit link. Both model formulations estimated the probability of SRKW occurrence by latitude and day of the year (DOY; 1-365) each year, but the specific handling of these covariates was different among candidate models. Both candidate models used a tensor product to estimate a two-dimensional smoothed surface for latitude and DOY. In addition, both model formulations included random effects for each station and fixed effects for each data source (MMET, SOBAD-Automated, SOBAD-Manual). The data source fixed effect allowed the model to account for potential differences between SoundTrap programming (continuous versus duty cycled) and data processing pipeline (manual versus automated), and their potential effects on the detection probability of SRKW. Longitude was not included as an effect, as the majority of SRKW monitoring occurred along a latitudinal gradient, except for SOBAD stations 12-15 and MMET stations JF and SS, all of which were positioned across a longitudinal gradient extending west from Cape Flattery and the Strait of Juan de Fuca. We therefore relied on station-level random effects to capture longitudinal variation in SRKW detection probabilities at these sites, all of which had very similar latitudes and would otherwise have been treated as having similar latitude-based detection probabilities by the models. The primary difference between candidate models was the handling of interannual variability. In the base model formulation (K_1), only a random effect of year was included, which would constrain the model to the same overall two-dimensional latitude–DOY occurrence pattern, but with higher or lower occurrence probabilities each year estimated by the random effect.

In the alternative model formulation (K_2) annual tensor products were estimated, meaning that the overall two-dimensional latitude – DOY occurrence patterns could be entirely different between years (Pedersen et al. 2019). Candidate models were fit using the mgcv package in R (Wood & Wood 2015, R Core Team 2024). Due to the large volume of input data, Fast Restricted Maximum Likelihood (fREML) was used to fit the models rather than the more common Restricted Maximum Likelihood (REML). AIC was used to select the model with the highest predictive performance. An overview of candidate model formulations used for SRKW data are presented in Table 6.

Table 6. Description of candidate generalized additive models for SRKW spatiotemporal analysis. tp = tensor product; re = random effect; fe = fixed effect. The top model based on the AIC score is indicated in bold and with *.

Model	Effects Included	Deviance Explained	AIC
K_1	tp(Latitude, DOY) + re(Year) + re(Station) + fe(Source)	30.3%	-2993.02
K_2*	tp(Latitude, DOY) + tp(Latitude, DOY, by = Year) + re(Year) + re(Station) + fe(Source)	31.8%	**-3099.00***

3. Results

3.1 Chinook Tagging Stock Composition

From 2019-2024, a total of 498 tags were deployed on Chinook salmon in Alaska (n = 293) and Washington (n = 205). Tag deployment locations and the number of deployed tags at each location subsequently detected on the Washington Coast array are shown in Figure 2. A total of 108 tags were deployed on Interior Ocean-type Chinook and subsequently detected on the Washington Coast array; 37 on Interior Stream-type Chinook; 6 on Oregon Coast Chinook; 1 on Southern OR / Northern CA Chinook; 6 on California Central Valley Chinook; 2 on Puget Sound / WA Coast Chinook; 7 on Northern British Columbia / SE Alaska Chinook; and 71 on Chinook from undetermined genetic origins (annual summaries in Tables 7 & 8).

Table 7. Summary of acoustic tags deployed on Chinook salmon from each stock aggregate in each year, 2019-2024. Note that cells indicate the number of tags deployed that were subsequently detected at least once in the Washington Coast array from 2019 to 2024. Tags that were never detected are not included here. Tagged salmon with undetermined stock aggregates in 2024 are currently pending results of genetic stock origin assignment.

Stock Aggregate	2019	2020	2021	2022	2023	2024
Interior Ocean-type	89	2	2	15	0	0
Interior Stream-type	30	1	2	4	0	0
Oregon Coast	2	0	0	4	0	0
Southern OR / Northern CA	1	0	0	0	0	0
California Central Valley	6	0	0	0	0	0
Puget Sound / WA Coast	2	0	0	0	0	0
Northern BC / Alaska	0	0	3	4	0	0
Undetermined	0	0	0	8	1	62

Table 8. Summary of tagged Chinook salmon detected from each stock aggregate in each year, 2019-2024. Cells indicate the number of tags from each stock aggregate that were detected at least once in the Washington Coast array in each year. Tagged salmon with undetermined stock aggregates in 2024 are currently pending results of genetic stock origin assignment.

Stock Aggregate	2019	2020	2021	2022	2023	2024
Interior Ocean-type	89	87	89	19	19	19
Interior Stream-type	30	26	28	7	7	7
Oregon Coast	2	2	2	4	4	4
Southern OR / Northern CA	1	1	1	0	0	0
California Central Valley	6	6	6	0	0	0
Puget Sound / WA Coast	2	2	2	0	0	0
Northern BC / Alaska	0	0	3	7	7	7
Undetermined	0	0	0	8	9	71

3.2 Chinook Detection Overview

A total of 101,026 receiver-days of effort were captured between 2019 and 2024 (i.e., the total number of days of active recording effort per receiver, summed across all receivers). 238 tagged Chinook salmon were detected a total of 4,269 times during this period, with each detection representing a unique day on which a tagged individual was recorded on one receiver. Standardized detection patterns of all tagged Chinook combined are presented in Figure 4; detection patterns for the Interior Ocean-type stock aggregate are shown in Figure 9. Across all tagged Chinook, the highest number of detections was recorded along the central to northern coast of Washington during the summer months, particularly in 2019 (Figure 4). In 2022, detection rates were highest near the Strait of Juan de Fuca and the Columbia River during summer months. In 2024, detections were highest along the southern Washington coast. Tagged Interior Ocean-type Chinook showed very similar detection patterns to those of the overall dataset, as they comprised the largest stock aggregate (Figure 9). However, the genetic stock identification of salmon tagged in 2024 remains pending, and these fish largely drove the detection patterns across tagged Chinook in 2024 (Figures 4).

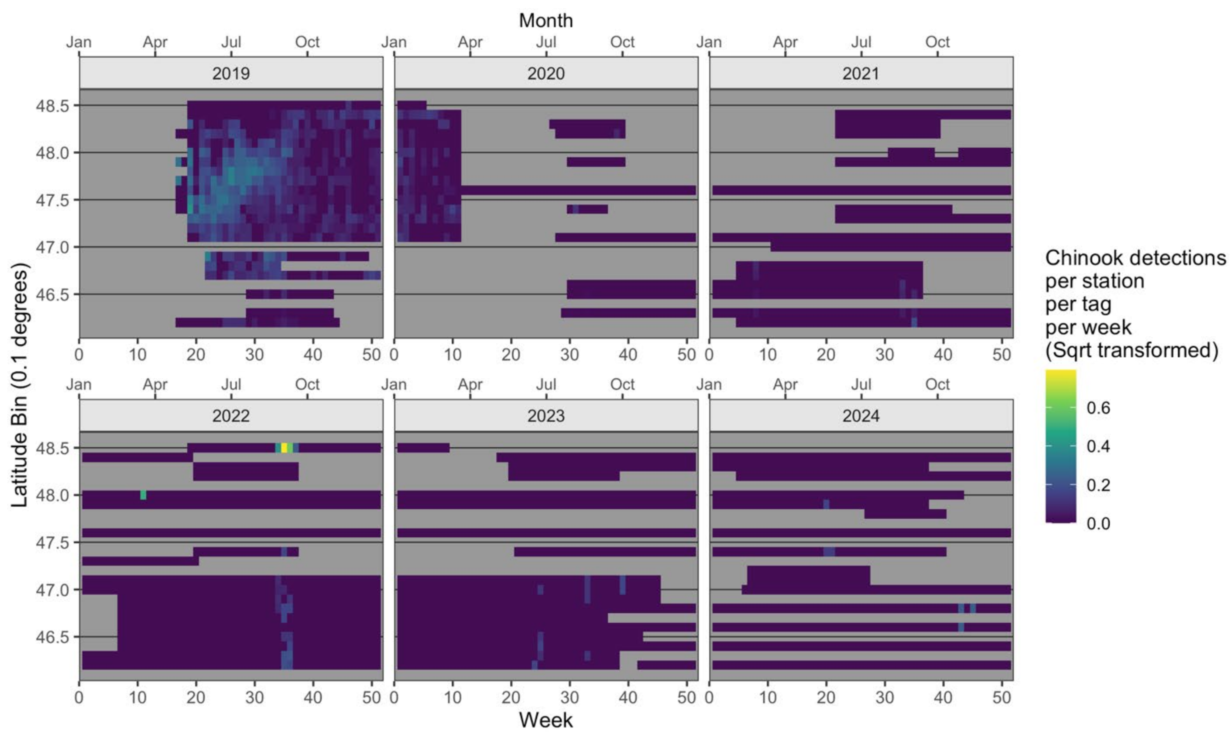

Figure 9. Standardized detection days of 69 kHz acoustic tags implanted in Chinook salmon from the Interior Ocean-type genetic stock aggregate, 2019-2024. Detections are standardized for effort by combining all active 69 kHz receivers into 0.1 degree latitudinal bins and dividing the number of days with tag detections for each receiver within a latitudinal bin by the number of active receivers and the number of active tags (from the Ocean Type stock aggregate only) for each calendar week. The resulting number of standardized detection days is then square-root transformed to improve the visibility of the detection gradient at lower values.

3.2 Chinook Spatial Modeling Results

The GAM including annual tensor products (model C_2/O_2) was the best supported model for both Chinook analyses (all tags, and Interior Ocean-type tags only) based on AIC scores (Tables 2 and 3). The mean tensor product of latitude and DOY can be interpreted as the average distribution of Chinook, integrating data across all years (Figures 10 and 11). In the combined tag model, Chinook had the highest probability of presence in the northern central coast (~47.5º latitude), with two peaks in early spring and early summer. An additional, lower peak occurred in the Strait of Juan de Fuca in the winter, and another on the southern central Washington coast in mid-summer (Figures 10 and 11).

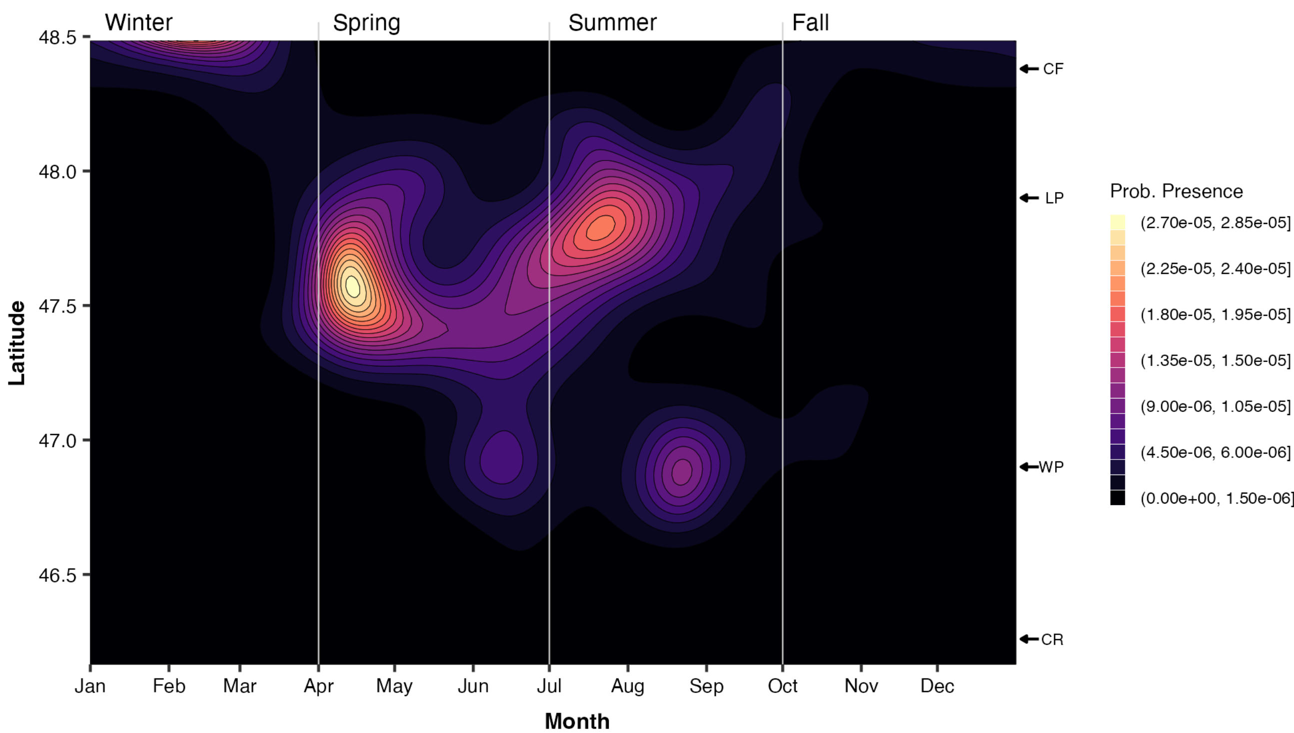

Figure 10. Model-estimated daily probability of tagged Chinook salmon presence (all tags combined) by latitude (y-axis) and day of the year (x-axis). Values are predicted using the overall mean tensor product from model C2, with no annual tensor products applied, and random effects of station and year withheld. Geographic locations of interest are indicated with arrows on the right side of the plot: CR = Columbia River; WP = Westport; LP = La Push; CF = Cape Flattery.

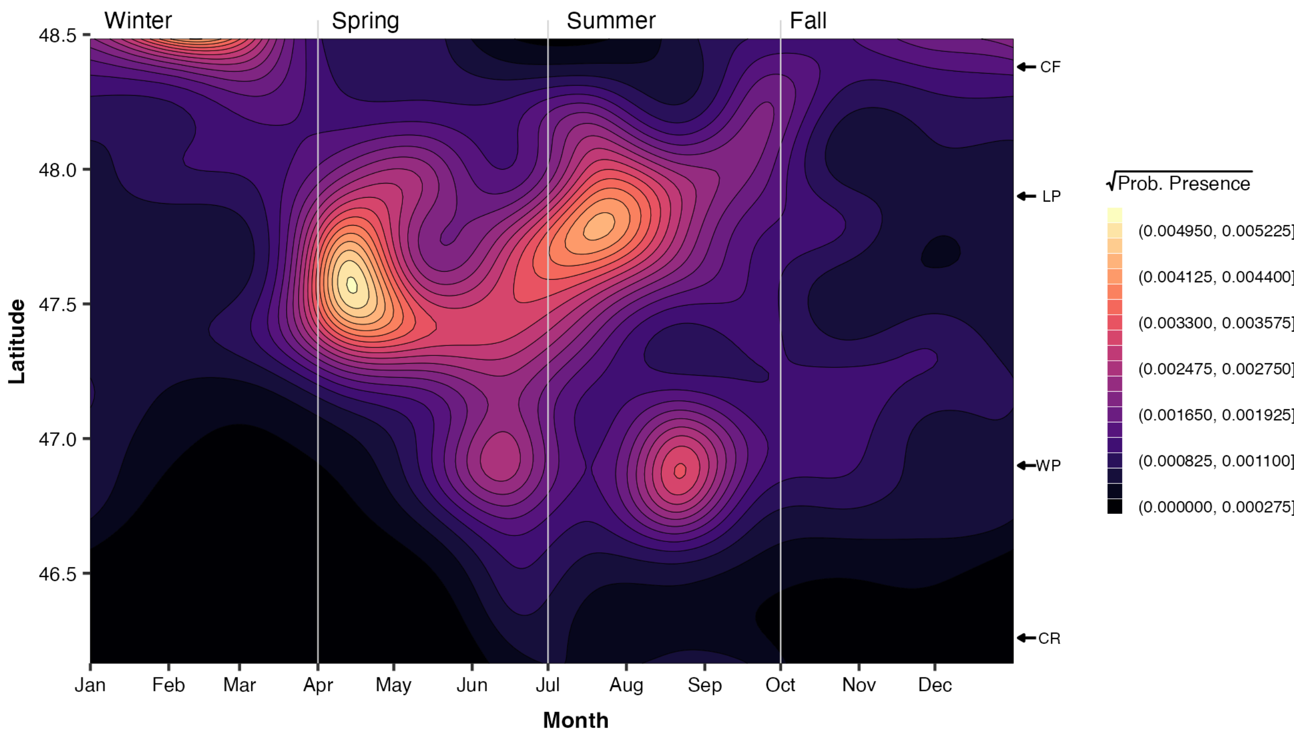

Figure 11. Model-estimated daily probability of tagged Chinook salmon presence (all tags combined; square root transformed) by latitude (y-axis) and day of the year (x-axis). Estimates are identical to those presented in Figure 10, but are square root transformed for improved visibility of the probability gradient across lower values. Values are predicted using the overall mean tensor product from model C2, with no annual tensor products applied, and random effects of station and year withheld. Geographic locations of interest are indicated with arrows on the right side of the plot: CR = Columbia River; WP = Westport; LP = La Push; CF = Cape Flattery.

Annual estimated patterns of occurrence varied substantially and may represent differences in the stock composition of tagged Chinook each year (Figure 12). 2019 and 2023 had similar patterns to the overall estimated distribution. In 2020, detection probability was concentrated in the southern-central coast in late spring. In 2021 and 2024, detection probabilities were high near the Columbia River mouth in late summer and along the southern coast from summer to mid/late fall. In 2021 and 2022, detection probabilities were high along the central and north-central coasts in early spring.

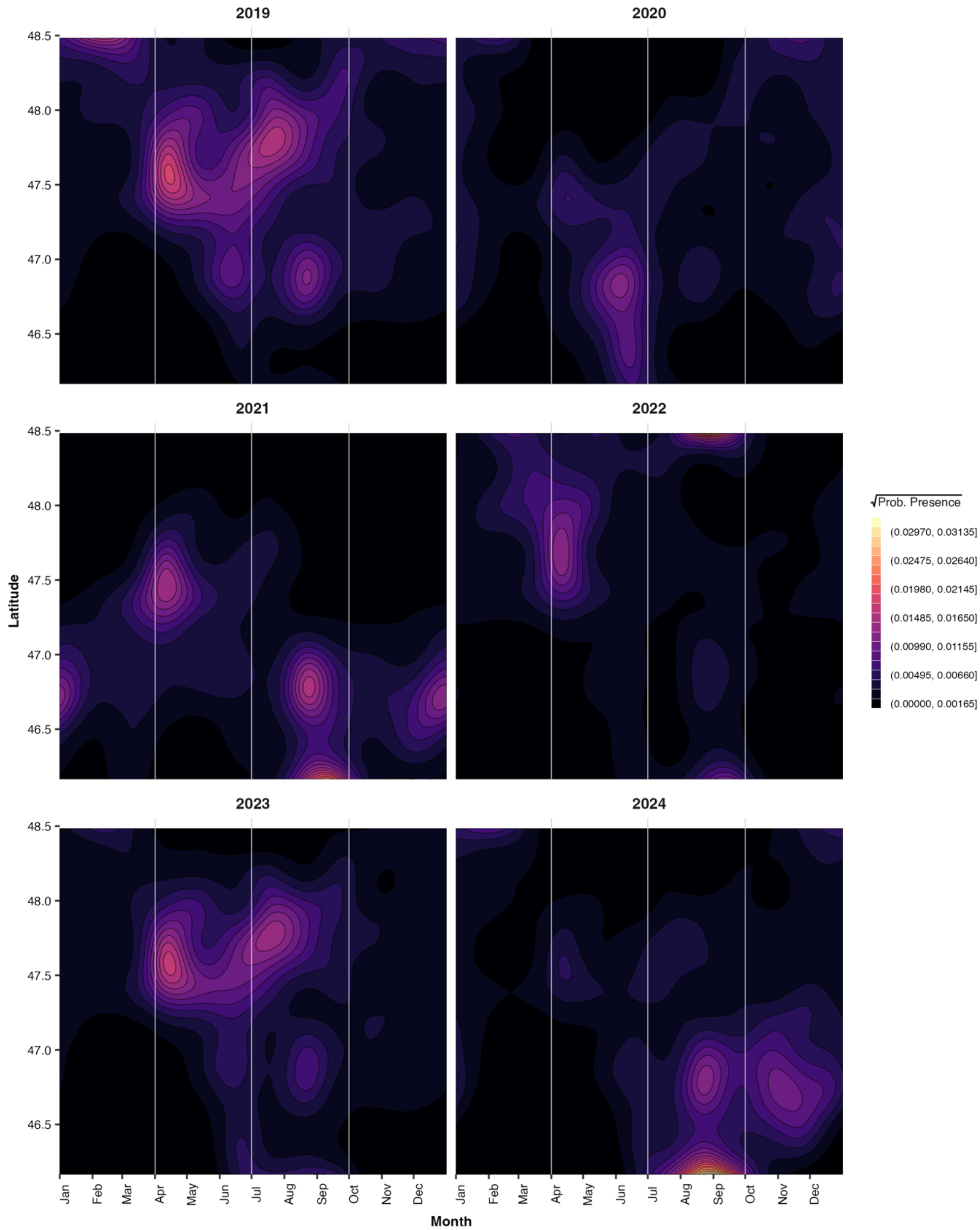

Figure 12. Model-estimated daily probability of tagged Chinook salmon presence (all tags combined; square root transformed) by latitude (y-axis) and day of the year (x-axis), for each year 2019-2024. Estimates are square-root transformed to improve visibility of the probability gradient at lower values (untransformed values are not shown). Values are predicted using the overall mean tensor product, plus annual tensor products and annual random effects from model C2, with station random effects withheld.

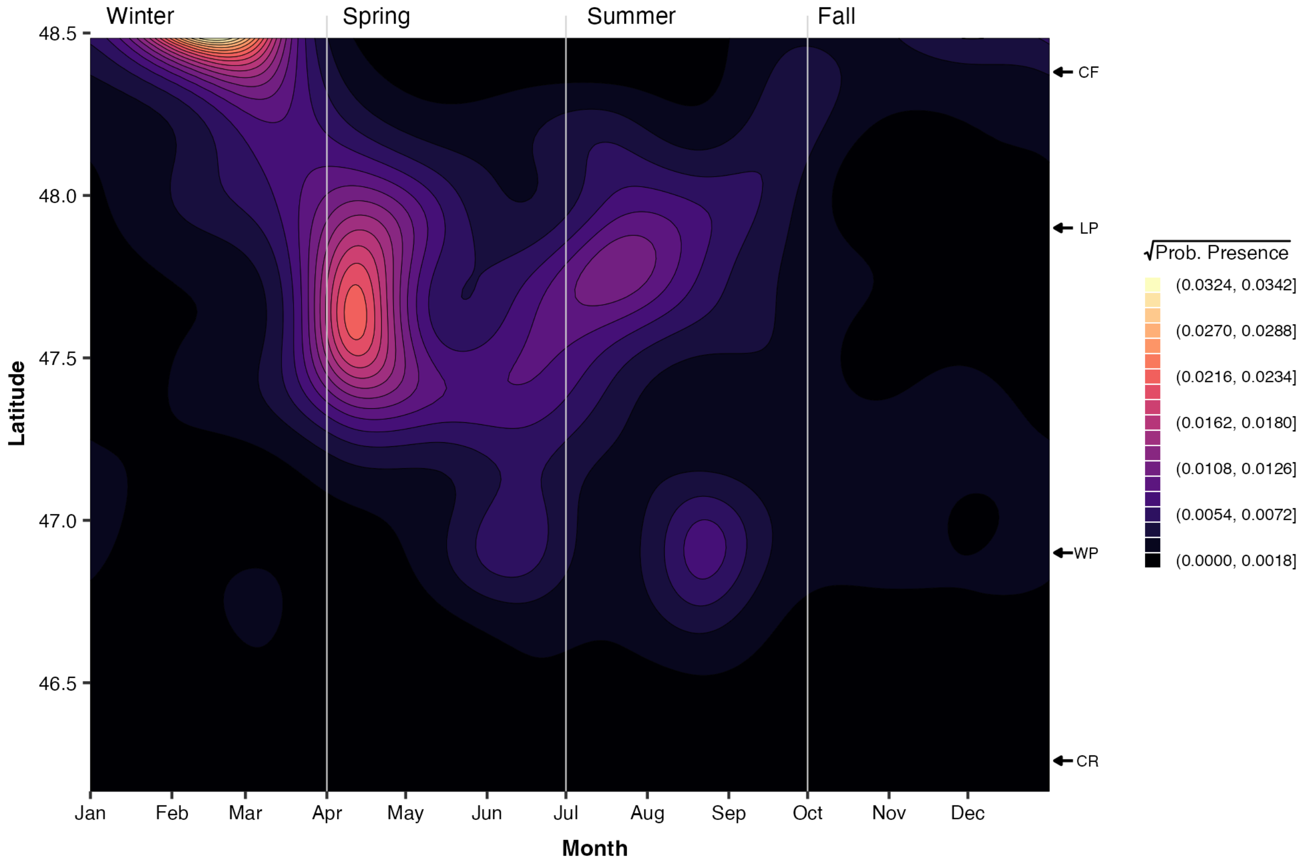

Figure 13. Model-estimated daily probability of tagged Interior Ocean-type Chinook salmon presence (square root transformed) by latitude (y-axis) and day of the year (x-axis). Estimates are square-root transformed to improve visibility of the probability gradient at lower values (untransformed values are not shown). Values are predicted using the overall mean tensor product from model O2, with no annual tensor products applied, and random effects of station and year withheld. Geographic locations of interest are indicated with arrows on the right side of the plot: CR = Columbia River; WP = Westport; LP = La Push; CF = Cape Flattery.

The Interior Ocean-type model showed the highest overall probability of occurrence in the Strait of Juan de Fuca during the winter months and on the north-central Washington coast in early spring (Figure 13). Annual patterns of occurrence varied substantially (Figure 14), with tagged Chinook occurrence shifting from the Strait of Juan de Fuca in winter to the north-central coast in spring in 2019, 2022, and to a lesser extent in 2024. In 2020, tagged Chinook had high detection probabilities near the mouth of the Columbia River in early spring. There were very low detection probabilities centered on the southern coast in the summer months of 2021 and 2023, and similar patterns with higher detection probabilities in 2024. In 2022, detection probabilities were high in the Strait of Juan de Fuca in late summer.

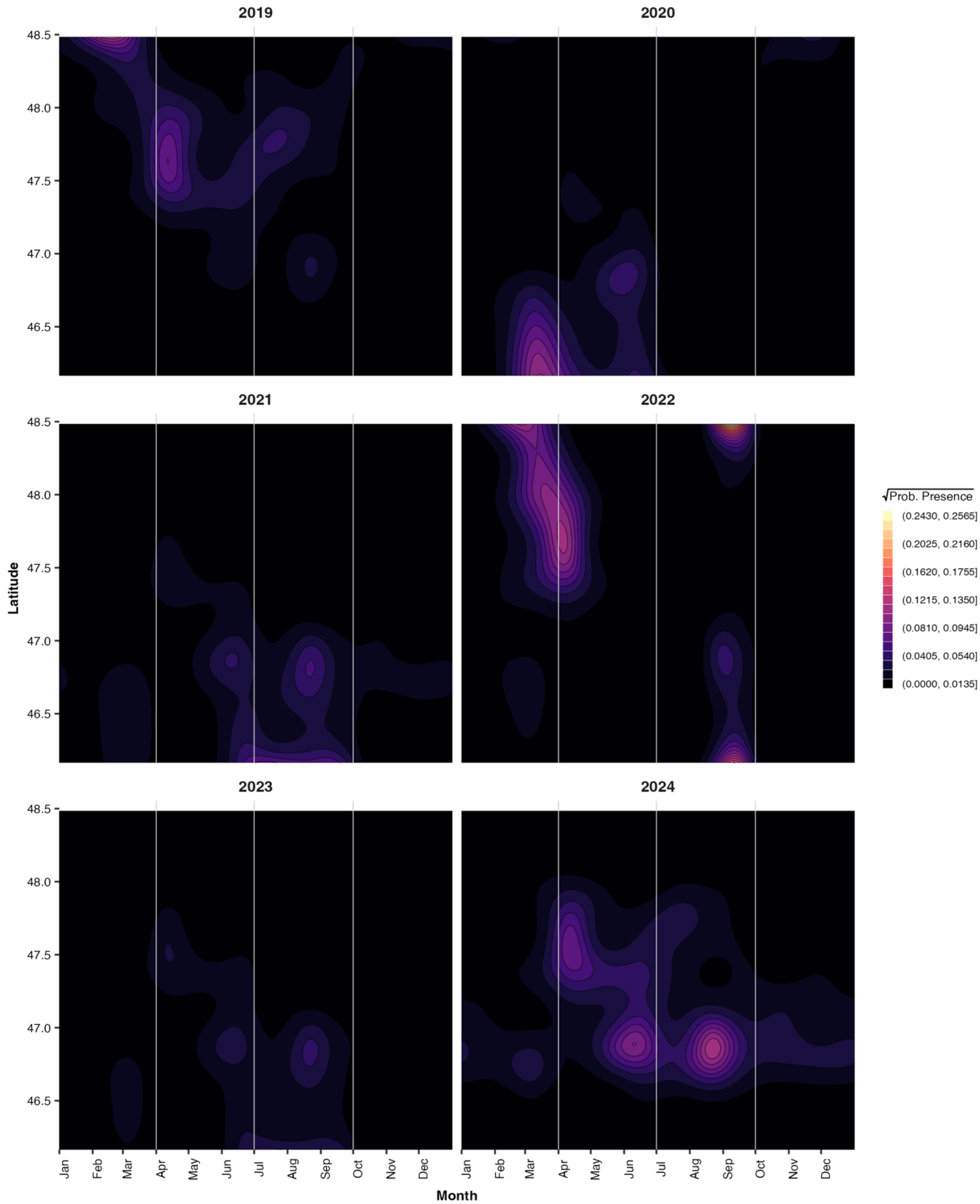

Figure 14. Model-estimated daily probability of tagged Interior Ocean-type Chinook salmon presence (square root transformed) by latitude (y-axis) and day of the year (x-axis), for each year 2019-2024. Estimates are square-root transformed to improve visibility of the probability gradient at lower values (untransformed values are not shown). Values are predicted using the overall mean tensor product, plus annual tensor products and annual random effects from model O2, with station random effects withheld.

3.4 SRKW Detection Overview

From 2018 to 2024, MMET SoundTraps had recording effort on 8,305 days across five mooring locations, and detected SRKW on 900 recording-days (i.e., one day of recording effort at one mooring location). In 2023 and 2024, SOBAD SoundTraps had recording effort on 5,016 days across 15 mooring locations, and detected SRKW on 378 recording-days. SRKW presence was highest during the summer and early fall months at northern stations near the Strait of Juan de Fuca (Figures 7 & 8). The mean number of SRKW presence days per week was highest at the MMET Swiftsure South (SS) and Juan de Fuca (JF) stations (2.69 and 1.97 days per week, respectively), and at SOBAD stations 14 and 15 (1.59 and 1.16 days per week, respectively). During the summer months only (June through September), these same four stations had the highest SRKW presence: 4.57 days per week (SS), 3.90 (JF), 2.61 (14), and 1.68 (15). The stations with the lowest mean SRKW detection days per week were SOBAD stations 6 and 1 (0.05 and 0.08 days per week, respectively) and MMET stations LP and CR (0.11 and 0.14 days per week, respectively). Across all years and all SoundTrap stations, the prevailing pattern of SRKW detections showed the highest probability of occurrence near the Strait of Juan de Fuca and Swiftsure Bank during summer and early fall months, and a much lower probability of occurrence from Westport south, peaking during early spring (Figure 8).

3.5 SRKW Spatial Modeling Results

The GAM including annual tensor products with independent wiggliness (model K_2), was the best supported model for the SRKW analysis based on AIC scores (Table 6). The mean tensor product of latitude and DOY can be interpreted as the average distribution of SRKW, integrating data across all years (Figures 15 & 16). SRKW had the highest probability of presence in the far north of the study area, near Cape Flattery and the Strait of Juan de Fuca (SJF), consistent with the raw detection data. Occurrence in this area peaked in the summer and early fall months, from July to November. In winter (December – early March), the occurrence probability in the SJF area was the highest in the study area but was considerably lower than during the summer months. From mid-March to early May, occurrence probability was highest for SRKW at the southern extent of the study area, near the mouth of the Columbia River. There were no significant differences ($p>0.05$) in detection probability by SoundTrap source (MMET, SOBAD manual detections, or SOBAD automated detections).

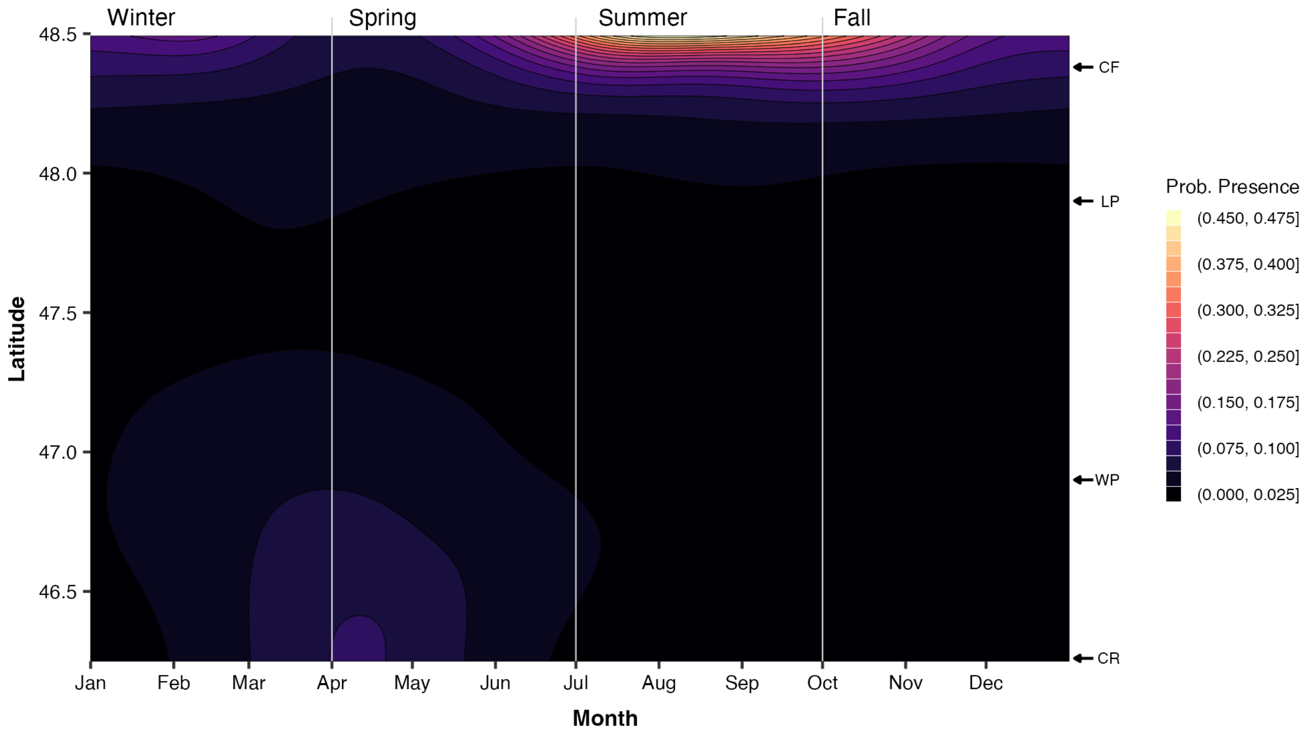

Figure 15. Model-estimated daily probability of SRKW presence by latitude (y-axis) and day of the year (x-axis). Values are predicted using the overall mean tensor product from model K2, with no annual tensor products applied, and random effects of station and year withheld. Geographic locations of interest are indicated with arrows on the right side of the plot: CR = Columbia River; WP = Westport; LP = La Push; CF = Cape Flattery.

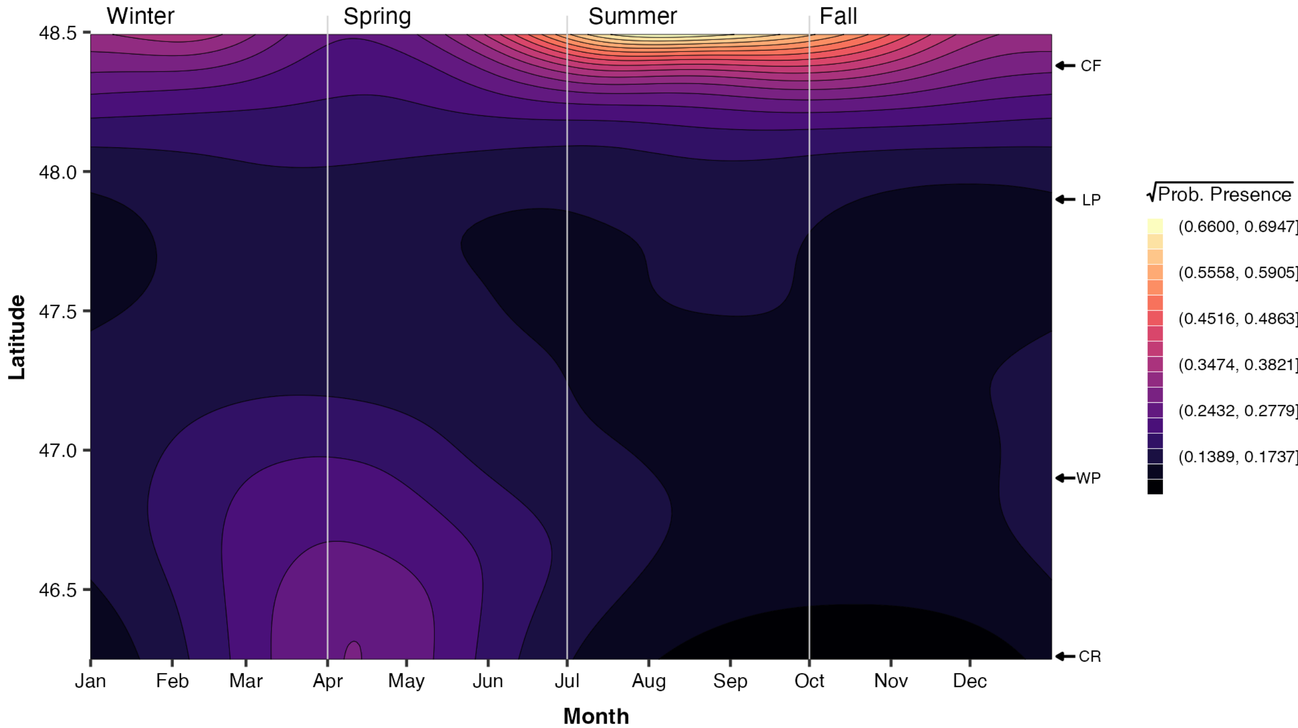

Figure 16. Model-estimated daily probability of SRKW presence (square root transformed) by latitude (y-axis) and day of the year (x-axis). Estimates are identical to those presented in Figure 15, but are square-root transformed to improve visibility of the probability gradient at lower values. Values are predicted using the overall mean tensor product from model K2, with no annual tensor products applied, and random effects of station and year withheld. Geographic locations of interest are indicated with arrows on the right side of the plot: CR = Columbia River; WP = Westport; LP = La Push; CF = Cape Flattery.

Annual patterns of estimated SRKW occurrence along the Washington Coast largely followed a similar pattern, with peak occurrence in the Strait of Juan de Fuca area during summer months, and moderate probability of occurrence near the Columbia River mouth during early spring. However, there was modest interannual variability in this prevailing pattern. For example, in 2019 the peak occurrence of SRKW in the Strait of Juan de Fuca area began later in the year, starting in October, and lasted longer into the winter months (Figures 17 & 18). In 2024, SRKW occurrence probability in the Strait of Juan de Fuca was lower during the early winter months compared with other years, and there was a higher probability of SRKW occurrence from Cape Flattery to central Washington during the summer. The timing of SRKW occurrence around the Columbia River was largely consistent across years, but the probability of occurrence varied, with the highest probability in 2023, moderate probabilities in 2018 and 2019, and lowest probabilities in 2020-2022 and 2024.

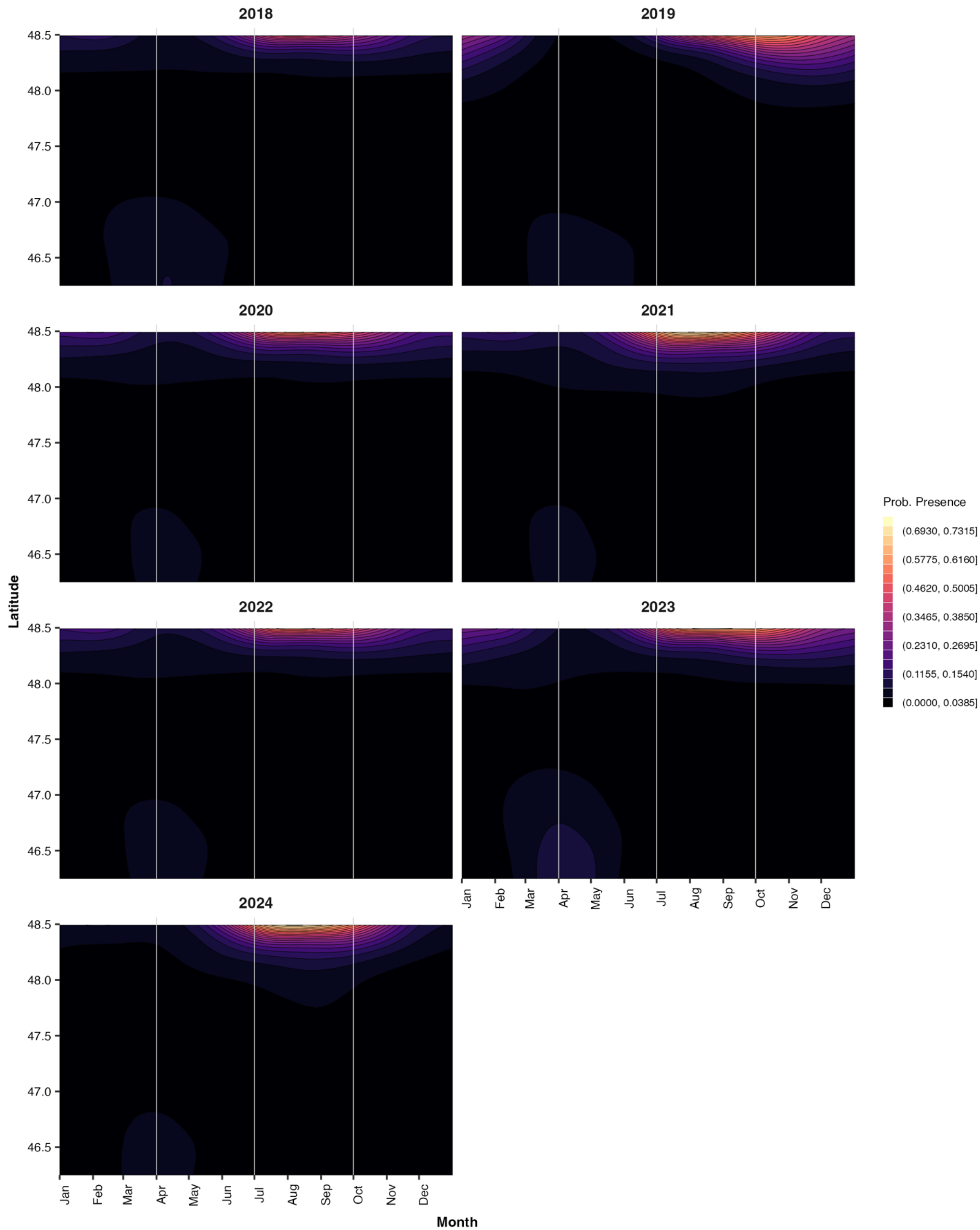

Figure 17. Model-estimated daily probability of SRKW presence by latitude (y-axis) and day of the year (x-axis), for each year 2018-2024. Values are predicted using the overall mean tensor product, plus annual tensor products and annual random effects from model K2, with station random effects withheld.

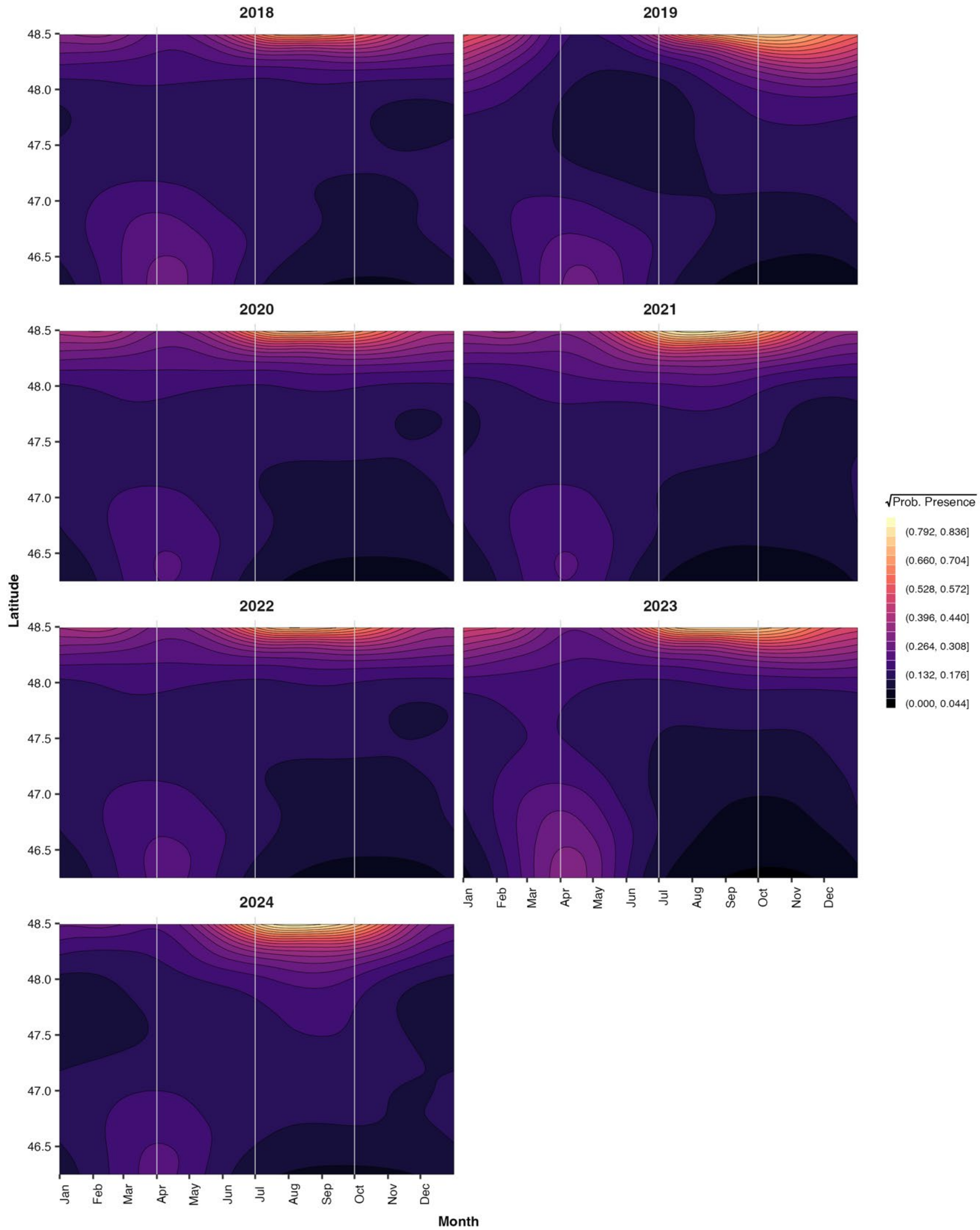

Figure 18. Model-estimated daily probability of SRKW presence (square root transformed) by latitude (y-axis) and day of the year (x-axis), for each year 2018-2024. Estimates are identical to those presented in Figure 17, but are square-root transformed to improve visibility of the probability gradient at lower values. Values are predicted using the overall mean tensor product, plus annual tensor products and annual random effects from model K2, with station random effects withheld.

4. Acknowledgments

Thanks to Joe Smith, Brian Wells, Brian Burke, Steve Corbett, and many other volunteers who helped with fish tagging, receiver deployment, retrieval, and downloading. Thanks to Doug Jackson for generating plots and assisting with data management, analysis, and interpretation. We appreciate the work by the staff at PMEL in mooring assembly and the efforts of the crews of the F/V Cape Windy, R/V Storm Petrel, and R/V Zephyr in the recovery and deployment of the moorings. Work inside the Olympic Coast National Marine Sanctuary was covered by permits OCNMS-2025-001 & OCNMS-2023-012. We thank Andrea Balla-Holden from the U.S. Navy, Pacific Fleet for providing funding to complete this study, Dr. Jessica Chen and Dr. James Powell from U.S. Navy, Naval Facilities Engineering Systems Command Pacific for comments on the report and logistics support, and Chris Hunt (ManTech) and Stephanie Sleeman (Naval Facilities Engineering Systems Command Pacific) for their review.

5. References

Center for Whale Research. 2026. https://www.whaleresearch.com/orca-population. Website accessed on 1/26/2026

DFO. 2025. Southern Resident Killer Whale Prey Selectivity in Relation to Chinook Salmon Stock and Size Composition within Canadian Critical Habitat. DFO Can. Sci. Advis. Sec. Sci. Advis. Rep. 2025/016.

Emmons, C. K., Hanson, M. B., & Lammers, M. O. 2021. Passive acoustic monitoring reveals spatiotemporal segregation of two fish-eating killer whale *Orcinus orca* populations in proposed critical habitat. *Endangered Species Research*, *44*, 253-261.

Ettinger, A. K., Harvey, C. J., Emmons, C., Hanson, M. B., Ward, E. J., Olson, J. K., & Samhouri, J. F. 2022. Shifting phenology of an endangered apex predator mirrors changes in its favored prey. *Endangered Species Research*, *48*, 211-223.

Ford, J. K. 1989. Acoustic behaviour of resident killer whales (*Orcinus orca*) off Vancouver Island, British Columbia. *Canadian Journal of Zoology*, *67*(3), 727-745.

Ford, J. K., Ellis, G. M., Barrett-Lennard, L. G., Morton, A. B., Palm, R. S., & Balcomb, K. C. 2006. Dietary specialization in two sympatric populations of killer whales (*Orcinus orca*) in coastal British Columbia and adjacent waters. Canadian Journal of Zoology, 84, 1084-1101.

Ford, J. K., Ellis, G. M., Olesiuk, P. F. & Balcomb, K. C. 2010. Linking killer whale survival and prey abundance: food limitation in the oceans' apex predator? *Biol. Lett.* **6**, 139–142.

Ghani, B., T. Denton, S. Kahl, and H. Klinck. 2023. Global birdsong embeddings enable superior transfer learning for bioacoustic classification. Scientific Reports 13:22876.

Hanson, M. B., Baird, R. W., Ford, J. K. B., Hempelmann-Halos, J., Van Doornik, D. M., Candy, J. R., ... & Ayres, K. L. 2010. Species and stock identification of prey consumed by endangered Southern Resident killer whales in their summer range. Endangered Species Research, 11, 69-82.

Hanson, M.B., Emmons, C.K., Ford, M.J., Everett, M., Parsons. K., Park, L.K., … $ Barre, L. (2021) Endangered predators and endangered prey: Seasonal diet of Southern Resident killer whales. PLoS ONE 16(3): e0247031.

Hanson, M., Emmons, C., Ward, E., Nystuen, J., & Lammers, M. 2013. Assessing the coastal occurrence of endangered killer whales using autonomous passive acoustic recorders. The Journal of the Acoustical Society of America, 134, 3486-95. https://doi.org/10.1121/1.4821206.

Hanson, M. B., Ward, E. J., Emmons, C. K., Holt, M. M., & Holzer, D. M. 2017. Assessing the movements and occurrence of southern resident killer whales relative to the US Navy's Northwest Training Range Complex in the Pacific Northwest. *Prepared for: US Navy, US Pacific Fleet, Pearl Harbor, HI. Prepared by: National Oceanic and Atmospheric Administration, Northwest Fisheries Science Center under MIPR*, *70*.

Holt, M.M., Tennessen, J.B., Hanson, M.B., Emmons, C.K., Giles, D.A., Hogan, J.T. and Ford, M.J., 2021. Vessels and their sounds reduce prey capture effort by endangered killer whales (*Orcinus orca*). Marine Environmental Research, 170, p.105429.

K. Lisa Yang Center for Conservation Bioacoustics. 2023. Raven Pro: Interactive Sound Analysis Software.

Kahl, S., C. M. Wood, M. Eibl, and H. Klinck. 2021. BirdNET: A deep learning solution for avian diversity monitoring. Ecological Informatics 61:101236.

Kardos, M., Zhang, Y., Parsons, K. M., A, Y., Kang, H., Xu, X., ... & Li, S. 2023. Inbreeding depression explains killer whale population dynamics. *Nature Ecology & Evolution*, *7*(5), 675-686.

Krahn, M. M., Hanson, M. B., Schorr, G. S., Emmons, C. K., Burrows, D. G., Bolton, J. L., ... & Wade, P. R. 2007. Persistent organic pollutants and stable isotopes in biopsy samples (2004/2006) from Southern Resident killer whales. Marine Pollution Bulletin, 54, 1903-1911.

Krahn, M. M., Hanson, M. B., Baird, R. W., Boyer, R. H., Burrows, D. G., Emmons, C. K., ... & Schorr, G. S. 2009. Effects of age, sex and reproductive status on persistent organic pollutant concentrations in "Southern Resident" killer whales. Marine Pollution Bulletin, 58, 1522-1529.

Ligges, U., S. Krey, O. Mersmann, and S. Schnackenberg. 2023. tuneR: Analysis of Music and Speech.

National Marine Fisheries Service. 2008. Recovery Plan for Southern Resident Killer Whales (*Orcinus orca*). National Marine Fisheries Service, Northwest Region, Seattle, Washington.

Oleson, E. and J. Hildebrand. 2012. Marine mammal demographics off the outer Washington coast and near Hawaii. NPS-OC-12-001CR, Naval Postgraduate School, Monterey, California.

Olson, J. K., Wood, J., Osborne, R. W., Barrett-Lennard, L., & Larson, S. 2018. Sightings of southern resident killer whales in the Salish Sea 1976–2014: the importance of a long-term opportunistic dataset. *Endangered Species Research*, *37*, 105-118.

Pedersen, E. J., Miller, D. L., Simpson, G. L., & Ross, N. 2019. Hierarchical generalized additive models in ecology: an introduction with mgcv. *PeerJ*, *7*, e6876.

Pilkington, J. F., Stredulinsky, E. H., Gavrilchuk, K., Thornton, S. J., Ford, J. K., & Doniol-Valcroze, T. 2023. Patterns of winter occurrence of three sympatric killer whale populations off eastern Vancouver Island, Canada, based on passive acoustic monitoring. *Frontiers in Marine Science*, *10*, 1204908.

R Core Team. 2024. R: A language and environment for statistical computing. R Foundation for Statistical Computing, Vienna, Austria.

Riera, A., Pilkington, J.F., Ford, J.K.B., Stredulinsky, E.H., and Chapman, N.R. 2019. Passive acoustic monitoring off Vancouver Island reveals extensive use by at-risk

Resident killer whale (*Orcinus orca*) populations. Endangered Species Research 39: 221-234.

Stewart, J.D., Durban, J.W., Fearnbach, H., Barrett-Lennard, L.G., Casler, P.K., Ward, E.J. and Dapp, D.R., 2021. Survival of the fattest: linking body condition to prey availability and survivorship of killer whales. Ecosphere, 12(8), p.e03660.

Stewart, J.D., Cogan, J., Durban, J.W., Fearnbach, H., Ellifrit, D.K., Malleson, M., Pinnow, M. and Balcomb, K.C., 2023. Traditional summer habitat use by Southern Resident killer whales in the Salish Sea is linked to Fraser River Chinook salmon returns. Marine Mammal Science, 39(3), pp.858-875.

Tennessen, J.B., Holt, M.M., Wright, B.M., Hanson, M.B., Emmons, C.K., Giles, D.A., Hogan, J.T., Thornton, S.J. and Deecke, V.B., 2024. Males miss and females forgo: Auditory masking from vessel noise impairs foraging efficiency and success in killer whales. Global Change Biology, 30(9), p.e17490.

Van Cise, A. M., Hanson, M. B., Emmons, C., Olsen, D., Matkin, C. O., Wells, A. H., & Parsons, K. M. 2024. Spatial and seasonal foraging patterns drive diet differences among north Pacific resident killer whale populations. *Royal Society Open Science*, *11*(9), rsos240445.

Ward, E. J., Holmes, E. E., & Balcomb, K. C. 2009. Quantifying the effects of prey abundance on killer whale reproduction. *Journal of Applied Ecology*, *46*(3), 632-640.

Wasser, S. K., Lundin, J. I., Ayres, K., Seely, E., Giles, D., Balcomb, K., ... & Booth, R. K. 2017. Population growth is limited by nutritional impacts on pregnancy success in endangered Southern Resident killer whales (*Orcinus orca*). PLoS ONE, 12, e0179824.

Wiggins, S. M., Roch, M. A., & Hildebrand, J. A. 2010. TRITON software package: analyzing large passive acoustic monitoring data sets using MATLAB. *The Journal of the Acoustical Society of America*, *128*(4_Supplement), 2299-2299.

Wood, S., & Wood, M. S. 2015. Package 'mgcv'. *R package version*, *1*(29), 729.